TRIBHUVAN UNIVERSITY

DEPARTMENT OF MECHANICAL AND AEROSPACE ENGINEERING

PULCHOWK CAMPUS, LALITPUR

B-14-BAS-2018/23

DESIGN AND FABRICATION OF AUTONOMOUS FIXED-WING UAS FOR MEDICAL SUPPLIES DELIVERY

by

Mandeep Prasad Shah (075AER021)

Pravesh Bhandari (075AER032)

Shankar Malla (075AER039)

A PROJECT REPORT

SUBMITTED TO THE DEPARTMENT OF MECHANICAL AND AEROSPACE ENGINEERING IN PARTIAL FULFILLMENT OF THE REQUIREMENT FOR THE DEGREE OF BACHELOR IN AEROSPACE ENGINEERING

DEPARTMENT OF MECHANICAL AND AEROSPACE ENGINEERING

LALITPUR, NEPAL

MARCH 2023

COPYRIGHT

TRIBHUVAN UNIVERSITY

INSTITUTE OF ENGINEERING

CENTRAL CAMPUS PULCHOWK

DEPARTMENT OF MECHANICAL AND AEROSPACE ENGINEERING

The undersigned certify that they have read, and recommended to the Institute of Engineering for acceptance, a project report entitled **"Design and fabrication of fixed wing UAS for medical supplies delivery"** submitted by Pravesh Bhandari, Shankar Malla, and Mandeep Prasad Shah in partial fulfillment of the requirements for the degree of Bachelor of Aerospace Engineering.

Supervisor: **Ashish Karki,**
Assistant Professor
Department of Mechanical and Aerospace Engineering
Institute of Engineering, Pulchowk Campus

External Examiner: **Sanjiv Paudel,**
Managing Director, Machine Hub Nepal

Committee Chairperson: **Dr. Surya Prasad Adhikari,**
Associate Professor
Department of Mechanical and Aerospace Engineering
Institute of Engineering, Pulchowk Campus

Date

ABSTRACT

The objective of this project is to develop a cost-effective and efficient Unmanned Aerial System (UAS) that can be utilized to transport medical supplies to remote and hard-to-reach locations. The UAS is a fixed-wing aircraft that is equipped with a parachute system for the safe and secure delivery of medical supplies. The design process includes the optimization of aerodynamic characteristics, flight dynamics, payload capacity, and the parachute deployment mechanism to ensure successful delivery. Additionally, the UAS has been designed to have a high lift capacity, allowing it to cross challenging terrains with ease.

The fabrication process of the UAS is underway, and this project will provide an update on the progress and highlight the key challenges faced during the development phase. The focus of the project is on ensuring that the UAS is capable of performing its mission effectively and efficiently.

This project aims to improve access to essential medical supplies in times of crisis and enhance the efficiency of medical supply chain operations. By providing a cost-effective and efficient delivery mechanism, we hope to help alleviate the burden faced by healthcare workers in remote locations and improve the overall quality of aid provided to patients in need.

Keywords: UAS, payload delivery, remote locations, aerodynamics, flight dynamics, parachute, medical supply.

ACKNOWLEDGEMENT

We would like to express our sincere gratitude to the Department of Mechanical and Aerospace Engineering for providing us with the opportunity to undertake this project. We would like to acknowledge our indebtedness and a deep sense of gratitude to our supervisor Er. Aashish Karki for mentoring us in the academic and other technical aspects of our project. We express our gratitude to Assistant Professor Dr. Sudip Bhattarai for providing valuable technical insights for the betterment of our project. We are indebted to Er. Bikalpa Bomjan Gurung and Asst. Prof. Kamal Darlami for providing important feedback regarding faults and improvements in the design process of the fixed-wing UAV for this project.

Special thanks to Er. Biman Rimal for guiding us, providing necessary avionics and equipment.

We would like to thank IIEC Pulchowk for providing workspace and machinery equipment and DBF Pulchowk for lending their equipment.

Finally, we would like to thank our friends and both seniors/ juniors, for their support, encouragement, and suggestions throughout the project.

TABLE OF CONTENTS

LIST OF FIGURES

LIST OF TABLES

LIST OF ACRONYMS AND ABBREVIATIONS

UAS	Unmanned Aerial System
UAV	Unmanned Aerial Vehicle
ISTAR	Intelligence, Surveillance, Target Acquisition, and Reconnaissance
R&D	Research and Development
VTOL	Vertical Take-off and Landing
RMLH	Ram Manohar Lohia Hospital
PE	Polyethylene
EPS	Expanded Polystyrene
AB	Aerogel Blankets
PIR	Polyisocyanurate
MIT	Maximum Insulation Time
MAVSDK	Micro Aerial Vehicle Software Development Kit
RC	Radio Control
GCS	Ground Control Station
FMU	Flight Management Unit
VLOS	Visual Line of Sight
CNC	Computer Numerical Control
LASER	Light Amplification by Stimulated Emission of Radiation
DBF	Design Build Fly

Wh	Watt Hour
mAh	MiliAmpere Hour

CHAPTER ONE: INTRODUCTION

1.1 Background

During the initial phases of development of UAS technology, UASs were mainly designed to assist in military applications like ISTAR (Intelligence, Surveillance, Target Acquisition, and Reconnaissance). Such applications could include convoy protection, strike missions, electronic warfare, and even the use of UAS as decoys. These UASs are mostly very large and have performance capabilities equal to or better than manned aircraft. A few examples of such UAS can be Predator, Global Hawk, United 40, etc.

Nowadays, smaller Mini-UASs are taking the market and gaining popularity in both military and civilian purposes. Small UASs act as an eye in the sky. Mini UASs like Raven, Wasp AE, Scan Eagle, and Switchblade are being used and loved by on-field army personnel.

Recently, Mini-UASs are being mainly used for cinematography. Besides cinematography, mini UASs are being used in different fields like agricultural inspection, monitoring, and spraying pesticides and fertilizers. Big companies like Amazon and Walmart are developing UASs for cargo transportation. Other applications include civil purposes such as assisting fire-fighter crews, forest fire detection, search and rescue, power line inspections, geographical mapping, pollution mapping, road traffic surveillance and border patrol.

1.1.1 Use of UAS in Cargo Transportation

The concept of using UAS for cargo transportation has been around for quite a while now. However, there are only a few cases where UAS for logistics of medical supplies have developed to the level of implementation. The development of UAS technology in medical applications has been slower compared to its accelerating maturation in the fields of media, agriculture, infrastructure, inspection etc. [1]

However, we can find a considerably increasing interest in the use of UAS and automated systems in manufacture and supply chain logistics related to pharmacy. [2]

A huge demand for secure and cost effective transportation of many other medicinal materials such as organs for transplant, blood for transfusion and clinical samples for pathology also exists.[3]

1.2 Problem Statement

Nepal is a developing country. The road network within Nepal has not flourished well. Moreover, the hilly and mountainous regions of Nepal have steep terrains and difficult geographical distribution. These things altogether make road transportation a tough grind. Therefore, having a medical urgency could get close enough to be a nightmare if the immediate supply of medical goods is impeded by the long and challenging endeavor of road transportation.

1.3 Objectives

1.3.1 Main objective

To fabricate a UAS to carry consumable medical goods as payload to a health center located at a remote high-hill region of Nepal

1.3.2 Specific Objectives

- To build a fixed-wing UAS compatible with the Pixhawk (PX4) flight controller.
- To incorporate a thermally-insulated payload cargo to maintain the stringent temperature requirements of the medical supplies mainly consisting of medicines, vaccines or blood.
- To incorporate vibration/shock-resistant cargo compartments by the use of shock absorbing material(s)
- To analyze the effectiveness of the incorporated thermal insulation method in maintaining suitable temperature for the medical payload.

CHAPTER TWO: LITERATURE REVIEW

2.1 UAS Configurations

In the sense of Article 8 of the Eleventh Air Navigation Conference, an unmanned aerial vehicle or a UAV is “a pilotless aircraft which is flown without a pilot-in-command on-board and is either remotely and fully controlled from another place, be it ground, space or another aircraft, or programmed and fully autonomous.” This definition distinguished UAVs from other aerial systems. The more professionally accepted term for UAV is unmanned aerial systems (UAS), which implies UAV in conjunction with ground station and data link.

UAS can be classified on the basis of their physical configuration as either fixed-wing, rotary-wing or a mixed configuration such as ‘tilt-rotor’. Fixed-wing UAS are more appropriate to use when high speed is required. Because of the aerodynamic construction of the fixed-wing UAS, less drag is generated. Hence, it is possible to achieve high speed with fixed-wing setup.

2.1.1 Other pros of fixed-wing setup include:

- Easy maintenance

  Fixed-wing UAS are easy to service because of their less complicated build. One or more motors and control surfaces are the main elements that are likely to require maintenance.
- Longer duration of flight

  Fixed-wing UAS can generate lift from their wings. Due to which, they have the ability to glide without consuming battery power, to some extent. This allows less battery consumption and longer duration of flight.

2.1.2 Cons of Fixed-wing setup

Requirement of a runway or an alternative launching system for take-off. This makes such UAS inoperable in case any of such take-off facilities is not available.
Inability to hover in air.

A fixed-wing UAS needs to constantly move forward to sustain its flight. Due to which, it cannot hold its position at a fixed location. This makes it challenging to deliver the supplies at a precise location.

The hybrid (mixed) configuration such as a tilt-rotor UAS could be designed to mitigate the cons of fixed-wing UAS as they feature vertical take-off like a VTOL rotorcraft and cruise flight similar to the fixed-wing UAS. This could eliminate the need for a runway or any other launching system.

However, the main challenge in hybrid (mixed) configuration lies in the transition between the hover flight and the cruise flight wherein the airflow over the wings may get detached and it is difficult to maintain the control of the aircraft. [4]

According to findings from [5] the design of the autopilot for tilt-rotor UAS is very time consuming and difficult due to its varying dynamic characteristics that lead to nonlinearity in control techniques.

UASs can also be categorized on the basis of their implementations, as R&D, Combat, Reconnaissance, Logistics, Commercial and Recreational (civil). The UAS that carries medical supplies comes under Logistics UAS. The challenge which arise along with the application of the aircraft as logistics UAS is to achieve the balance between payload, range and flexibility. [6]

The use of UAS technology for medical logistics is emerging because of its range, performance, and cost effectiveness compared to other means of logistics such as ground vehicles, planes etc. Cost/benefit analysis done by [6] shows that the delivery of medical supplies using logistics UAS can be even cheaper than using Rickshaws for delivery.

On the contrary, the medical delivery service provider ‘Zipline’ experienced that their business is not more economic compared to the traditional means of transportation (i.e. by roads) as of 2017.[7]

Considering the gap between researches and evaluation of the actual systems in use, it should be kept in mind that that the cost analyses are inconclusive for the full evaluation of the economical aspect of medical logistics using UAS. [8]

We can find some contemporary examples of UAS which are being used for medicine delivery from the following illustration:

Site	Start	Company name	Product	Flight duration	Distance (one-way)	Maximum payload
Vanuatu S. Pacific	12/2018	Swoop Aero, Wingcopter	Vaccines	30 mins	45km	6kg
Rwanda and Ghana	10/2016	Zipline	Blood	30 mins	80km	1.8kg (3 units)
Tanzania	10/2018	DHL, GIZ &Wingcopter	Snake venom antiserum, etc.	40 mins	60km	6kg
Urban Switzerland	03/2017	Swiss Post, Matternet	Blood, test specimen	10 mins	3km	2kg
Rural Virginia	07/2015	Flirtey	Drug	3 mins	Not mentioned	5.5kg
Rural Madagascar	07/2016	Vayu	Blood and faeces test specimen	Not mentioned	Up to 60km	2kg
Rural China	06/2017	SF Technology	Injection	Not mentioned	Up to 15km	8kg

Figure 2. 1: Different Medical UAS and their Specifications [9]

2.2 Requisites for storage of some medical goods.

2.2.1 Blood

RMLH, India provides the following information on storage and transportation of blood.

Red blood cells and whole blood must be stored at a temperature between +2 ^{0}C to +6 ^{0}C. They should be issued in the blood transport box or insulation box which should keep the temperature under 10 ^{0}C. Similarly, the temperature range requirement for transporting Platelets is 20 ^{0}C to ^{0}C. It should be kept in mind that platelets should never be refrigerated.

Biological samples are very fragile; so the factors like high temperature, rapid acceleration and impact can destroy blood cells. [3] However, from the 33 common tests performed, [6] found no difference between the blood samples which have not been flown at all and 56 other blood samples which were flown via a fixed-wing UAV, after refrigeration.

2.2.2 Vaccines

The general precautions that should be considered to transport vaccines as given by [10] are as follows:

- Vaccines should be protected from shock, drop and vibrations.
- During transportation, the vials should be stored in an upright position.
- A set of cartons or vials should not be subjected to repeated transportation.

If a carton or a vial has been transported once, it should not be sent out again. It should rather be used at the arrival site, even if it has not been in transit for the maximum allowable period. This is a measure of precaution as it is difficult to keep track of the time that the particular vial has been under transportation.

AstraZeneca and Vero Cell are the most administered vaccines in Nepal, against Covid-19. These vaccines should be kept in a certain temperature range in order to maintain their efficacy. The requirements to consider for these vaccines are:

- Storage and transport conditions: +2 ^{0}C to +8 ^{0}C.
- Not to be frozen
- To protect from light

2.2.3 Medicines

The acceptable duration of storage at room temperature varies according to the nature of medicine. Some medicines would be effective for months while some may expire within a day if not refrigerated (Refrigeration temperature: 2 ^{0}C to 8 ^{0}C). Thus, the temperature conditions should be maintained according to particular medicine requirements. [11]

Temperature between 15°C and 30°C is allowed. [12] Transient spikes up to 40°C are permitted as long as the mean kinetic temperature does not exceed 25°, for a maximum time of 24 hours.[12] Spikes above 40° may be permitted only as per the instructions provided by the manufacturer and when there are not any specific instructions in the medicine's label, they must be always be protected from freezing temperature, moisture and excessive heat as well as from light during shipping and distribution, whenever necessary. [12]

2.3 Insulation Container

Insulated containers have a limited cold life i.e. the maximum time that the container can maintain the required temperature range. Most of such containers can maintain the temperature for a maximum time of three to four hours. However, other factors such as the external temperature, the frequency of opening and closing the container, the material used for packaging and the amount of vaccines being stored may alter the amount of time that the vaccines can be stored in the container. The temperature inside the container must be continually monitored during transportation. The frequency of checking the temperatures depend on the time the vaccine has been under storage and transportation inside the container. [10]

A thermally insulated cargo container usually contains one or more coolant pack(s) for temperature regulation inside the walls lined by insulating materials such as Polyethylene (PE), Expanded Polystyrene (EPS), Aerogel blankets (ABs), Polyisocyanurate (PIR) etc.

The shape of the gel packs plays a significant role in melting and absorption of the latent heat. The gel packs having large surface with small volume keep the product cooler but melt faster. On the other hand, the gel packs with smaller surface and larger volume melt slower but cannot keep the product as cold. [13]

The maximum insulation time (MIT) achieved by different materials used as insulating walls depend on various factors like emissivity, thermal conductivity, surrounding temperature, thickness etc. Increase in surface emissivity will cause less heat reflection and quicker transfer of heat through the walls, thus reducing the MIT. Materials like aluminum foil and PIR composite foil, which have remarkably low emissivity, can be integrated with other insulating materials to achieve better insulation of the container.

The experiments of [14] find that the MIT increases by 46% and 40% with aluminum foil applied on PE and EPS liners respectively, compared to the original PE and EPS packages. Whereas the increase in MIT per unit thickness by 79% and 106% is found for foiled PIR and AB insulated packages respectively, compared with the EPS insulated packages.

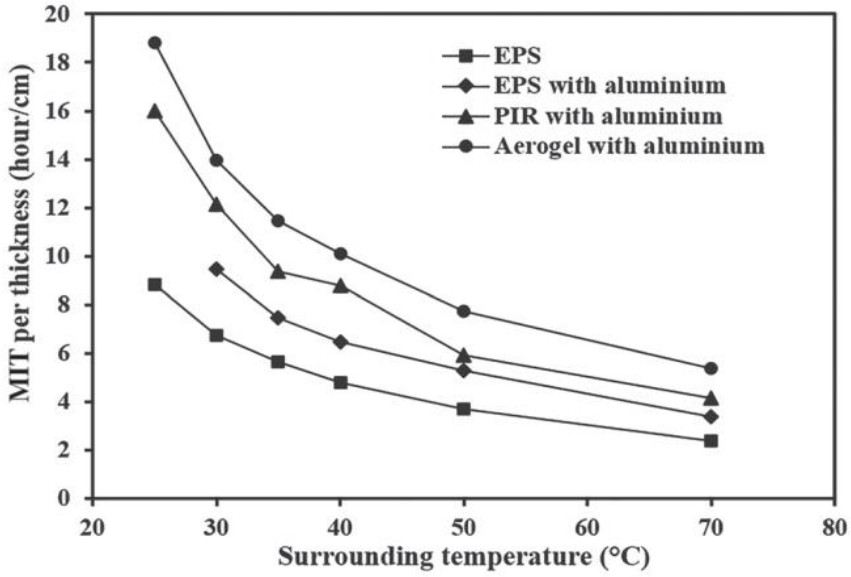

Figure 2. 2: Surrounding Temperature VS. MIT per unit thickness EPS, PIR, Aerogel packages [14]

2.4 Pixhawk 2.4.8 (PX4)

Pixhawk 2.4.8 is a popular open-source autopilot system designed for unmanned aerial vehicles (UAVs) and other robotic systems. Developed by the Pixhawk Project, this powerful flight controller offers advanced features and capabilities, making it a popular choice for DIY drone builders, researchers, and commercial drone operators alike.

The Pixhawk 2.4.8 offers a wide range of sensors and communication options, including GPS, barometer, magnetometer, and more. It also supports a variety of autonomous flight modes, such as waypoint navigation, circle mode, and return to home.

With its modular design and open-source software, the Pixhawk 2.4.8 allows for easy customization and integration with other systems, making it a versatile and flexible solution for a wide range of applications. Whether you're building a small quadcopter for recreational use or a large-scale drone for commercial operations, the Pixhawk 2.4.8 offers the performance and flexibility you need to get the job done.

Px4 supports a number of features and accessories that help improve the safety and performance of a UAS. Some of them are listed below:

- Radio Control (RC)
- SD Cards
- Safety Switch
- Data/Telemetry Radios
- GCS Joystick Controller
- Arming and Disarming
- Flight Modes (Autonomous and Manual)
- Failsafe systems

Some characteristic features of PX4 are listed below.

- 32-bit ARM Cortex M4 core with FPU
- 168 Mhz/256 KB RAM/2 MB Flash
- 32-bit failsafe co-processor
- On-board Sensors: Accelerometers, Gyroscope, Magnetometer, Barometer.
- Weight: 38 g
- Dimensions: 50x81.5x15.5 mm
- Operating Temperature: -40 to ~85 degree Celsius

Figure 2. 3: Pixhawk PX4 Flight Controller [18]

2.5 Economic Feasibility Analysis

This project requires the use of several hardware components which are costly to purchase. The most expensive hardware component required for our project is a flight controller. The department provided us with Pixhawk flight controller which significantly reduced the cost of fabrication. Moreover, the GPS Module, brushless motor, propeller blade, LiPo battery and Styrofoam blocks required for fabrication was also available for use, at the department. Due to the availability of LASER Cutter and 2-axis hot wire CNC cutter at the department, the cost for machining is also reduced. The components that should be bought are servo motors, tapes, laminate, plywood, screws, glue. Since, most of the components were taken off-the-shelf. The overall estimated cost of fabrication is 16,000 Rupees only. Thus, the grant provided for the project is sufficient to complete the project.

2.6 Relevant Research

2.6.1 Zipline at Rwanda

In Rwanda, a California-based company ‘Zipline’ commercially operates fixed-wing UASs to deliver medical supplies to 25 different clinics and hospitals across the country. [15] Zipline is the first in the world to offer regular delivery of emergency medical products. [7] Zipline’s autonomous UASs (drones) have a top speed of 128 km/h; range of 160 km and can carry up to 1.75 kg of cargo. The service radius from its distribution center is 75 km. [16]

Process of execution of the delivery [15]

When an order for medical goods is placed, the workers of Zipline wrap the supplies in padding and stuff the bundle into a bright red box, which is attached with a wax-paper parachute.

The red box and parachute are placed in the belly of the drone, whereas the battery pack is placed into the nose of the drone.

The drone is then placed on a 13-meters-long electric catapult that is powered by a bank of supercapacitors and is launched. Now the drone is fully autonomous.

After the drone reaches the destination, the package is parachuted and the drone returns to home.

Zipline’s landing system has two 10-meters-high towers, each having a vertically mounted rotating arm. A cable is strung between the arms such that a tiny metal hook below the tail of the drone returning to home gets stuck on the cable. When the drone is snagged, the rotating arm allows it to swing between the towers such that it comes to a stop within a few meters.

The drones of Zipline can carry payloads to longer distances than the rotorcrafts because they are fixed-wing aircrafts, which are aerodynamically more efficient than rotorcrafts. [15]

2.7 Research Gap

The use of UAS in logistics is developing rapidly and it is important to establish the framework and tools for proper handling of goods, especially medical products, to ensure their quality for consumption and safety for human health. [19]

Conventional stability considerations should be expanded to incorporate a wider range of stresses such as rapid changes in pressure and humidity, g-force, vibration and temperature excursions encountered during transportation of supplies via UAV, as they may impact the critical material attributes of the medicines. [19]

CHAPTER THREE: METHODOLOGY

3.1 Design procedure

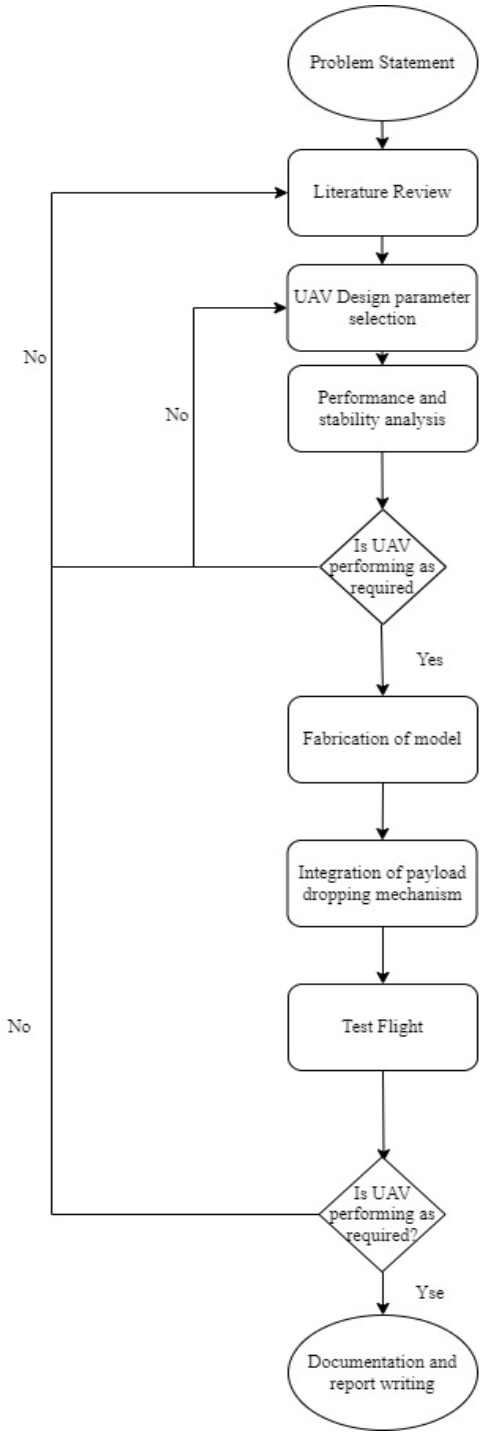

Figure 3. 1: Project detail flowchart

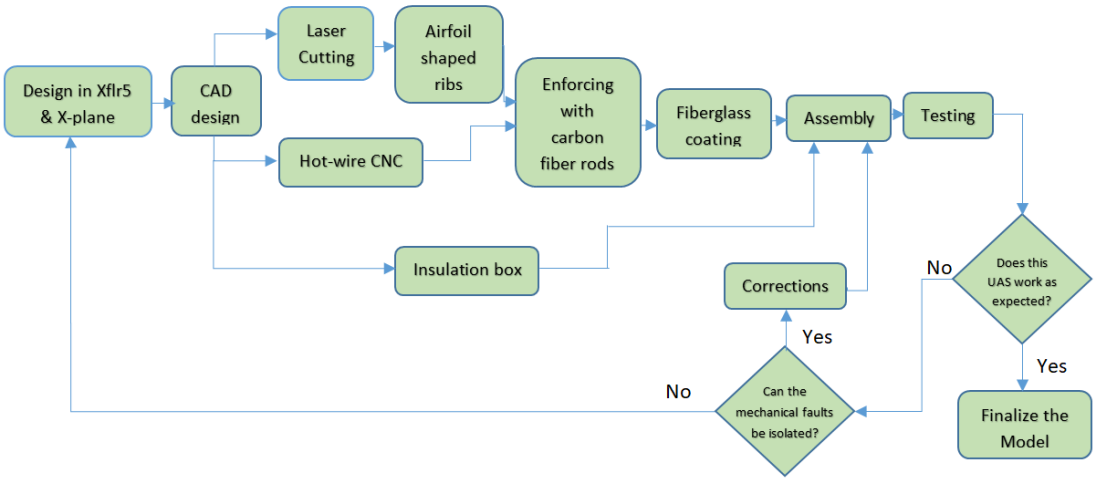

Figure 3. 2: Manufacturing Plan Flowchart

3.1.1 Collection of initial Data

We looked at the design parameters of different commercial and serviceable UASs that are available on the internet, for the initial sizing of the UAS for our project. Some of the common fixed wing UAS manufacturers are PENGUIN UAV, ALBATROSS UAV, FIXAR, CARBONIX etc.

3.2 Design

3.2.1 Mission Analysis

The UAV is designed to transport a maximum of two kilograms load of medical supplies which should occupy no more than 0.0045 m^3. The mission should address the immediate need of medical supplies demanded by health centers which have confirmed to the use of this UAV at the times of relevant medical emergencies. The mission includes loading of medical supplies like vials of vaccines and human blood from a blood bank, a pharmacy or a suitable medical reservoir; transporting it to the demand location in the form of a package which is dropped with parachute deployment, and then returning to the location where the UAV took-off.

To ensure the suitability of operation of the UAV in Nepal's hilly region, mainly the Shiwalik Range and the Mahabharat Range, the mission has been planned such that the selected location can incorporate the general terrain distribution of the region expected for operation therein. The selected representative location is Kushma Municipality of Parbat District and its outskirts.

Designing mission has been done by studying the distance between a medical supplier of Kushma Municipality (~850 m) and a primary health center located at Tilahar (~1100 m) , a rural village of Parbat, the obstacles in the nearest route between the two locations as well as the ascent and descent required to cover the mission.

The UAV will take-off at the altitude of 850 m with take-off run. Mission planning will be done with QGround Control Software. The UAV will autonomously climb to an altitude of 1000 m and cruise through fourteen kilometers until it reaches Tilahar. It will loiter close to the location where the package of medical supply needs to be dropped. After dropping the payload, the UAV will again set for a cruise flight back to the take-off location. It should cruise back maintaining an altitude of 1000 meters throughout. During final approach, it should descend to 900 m and then land on its landing gears. The landing gear will be down and extended throughout the mission.

Communication between the UAV and the ground station will be maintained with MAVLink Protocol. Meanwhile, the flight controller will record the flight data such as the actual flight path followed, speed and altitude in the SD card inserted within. After landing, the ground team will perform necessary maintenance actions.

Table 3. 1: Mission Phases

	Segment	**Description**
1	Take-off and Launch	Take-off distance 50 metres Take-off and launch speed 15 m/s
2	Turn	Turn radius= 100m
3	Climb	Climb to 1100 metres, 2m/s
4	Cruise acceleration	Range= 14 kms,

		Max Cruise Speed= 18 m/s
5	Turn	Turn Radius= 300 m
6	Loiter & Payload drop	Get within 10 m radius of Point of Payload drop
7	Cruise back	Range= 13 kms. Max Cruise Speed= 18 m/s
8	Descend	Descend rate= 3m/s
9	Land	Landing Distance= 60 m

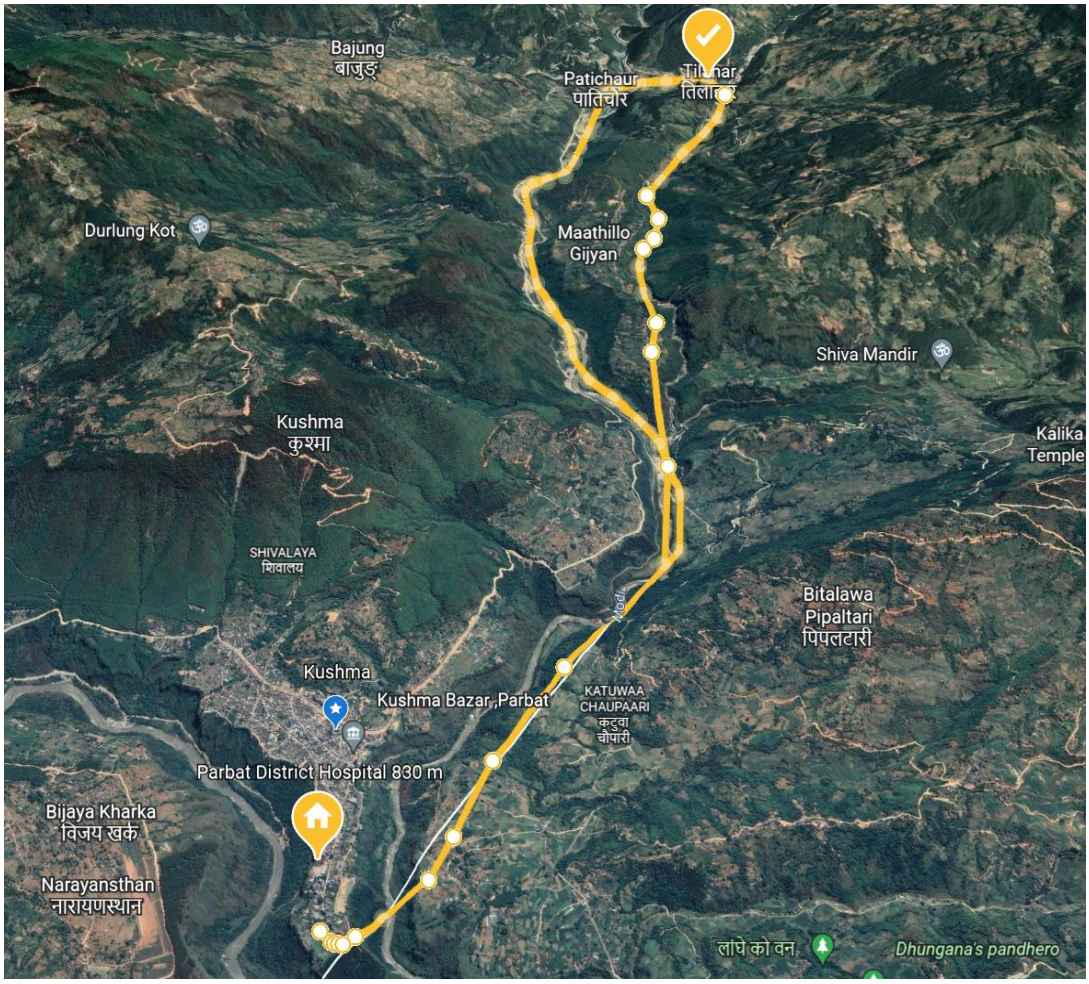

Figure 3. 3: Mission Location

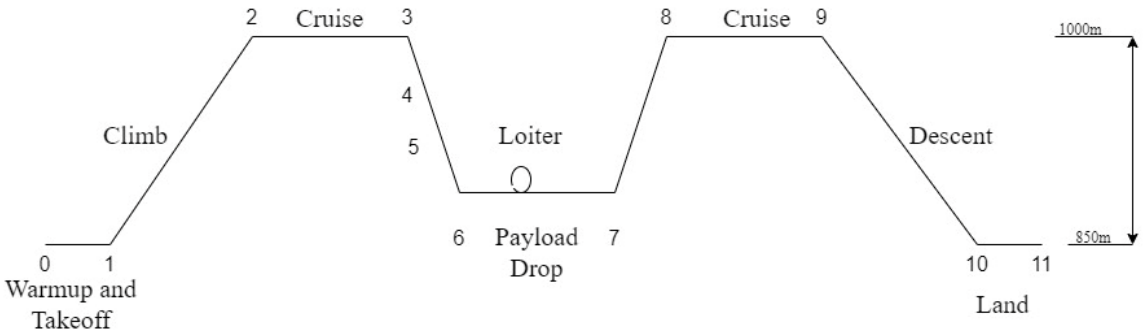

Figure 3. 4: Mission Profile

3.2.2 Initial Estimates

Wing Aspect Ratio

In this mission, the UAV has to fly through difficult landscapes and irregular terrain. This makes maneuverability an important requirement for the mission. Short and thick wings have greater maneuverability. For two different wings having same area but different aspect ratio, the amount air that can escape from bottom of the wing to the upper surface is higher for the wing with lower aspect ratio (Raymer, 2018).This escape reduces the lift at the tip and increases the drag due to lift. On the other hand, this reduces the effective angle of attack at the tip thus increasing the stalling angle. Again, to avoid terrains the UAV may have to perform quick steep climbs, which makes high stall angle a preferable choice for this mission. However, for the same wing area, a high aspect ratio wing suffers less loss of lift and increase in drag due to the formation of tip vortices. Since the mission involves flight over the hilly regions, the UAV will have need high lift to fly higher than the obstacles. Thus increase in lift to due increase in coefficient of lift is also important. For this, there should be high aspect ratio. Considering these trade-offs, the Wing Aspect Ratio is selected as 7.

Wetted Area Ratio

The parasitic drag of an aircraft depends on its total surface area directly exposed to air, known as its wetted area. The ratio of the wetted area to the reference area of the wing is known as the wetted area ratio. The wetted-area ratio and aspect ratio can be used together to initially estimate the aircraft's lift-to-drag ratio (L/D). From figure 7, it can be observed that the wetted-area ratio for single engine general aviation aircraft with conventional configuration is nearly equal to four. Hence, we estimate the wetted-area ratio for our UAV to be four.

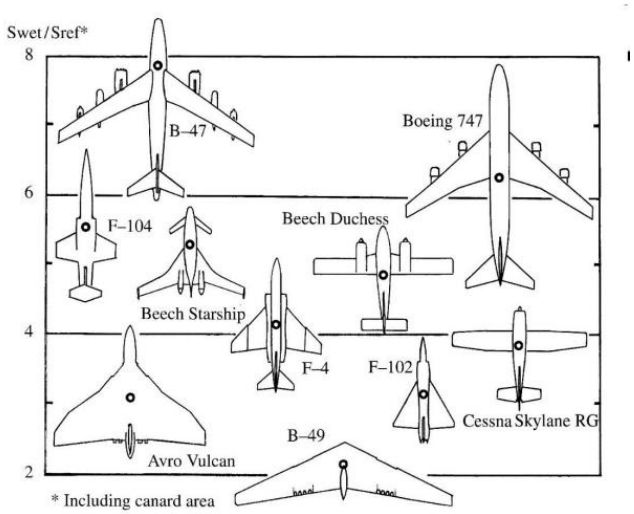

Figure 3. 5: Wetted Area Ratio of Real Aircrafts

Lift-to-drag ratio (L/D)

The initial estimate for lift-to-drag ratio for this UAV has been done with the help of historical data. At subsonic speeds, the lift-to-drag ratio is mostly affected by wetted area and wing span. L/D depends upon both the induced and parasitic drags. The induced drag largely depends upon the wing span whereas the parasitic drag depends on aircraft's wetted area. All these parameters can be incorporated in a new parameter called the wetted aspect ratio (A_{wetted}), which is the ratio of wing geometric aspect ratio to the wetted-area ratio.

A_{wetted} = Aspect Ratio / Wetted Area Ratio

= 7/4

= 1.75

$(L/D)_{max} = K_{LD} \sqrt{A_{wetted}}$

According to the data used in [17],

K_{LD} for non-retractable propeller aircraft = 9

$\therefore (L/D)_{max} = 11.9 \approx 12$

For propeller aircraft,

$(L/D)_{cruise} = (L/D)_{max} = 12$

$(L/D)_{loiter} = 0.866\ (L/D)_{max} = 10.4$

Stall Speed

To ensure the safety of flight especially during climb as well as approach, the maximum stall speed is estimated to be 15 m/s.

Take-off distance

The case adopted for this mission has ~120 m distance available for take-off. That is why the UAV should be designed for short take-off and landing (STOL). To ensure a successful take-off and obstacle clearance, the initial estimate for ground roll is 60 m.

3.2.3 Constraint Analysis

Drag Polar

Drag Polar depends on distinguishing features of an aircraft like its weight, shape and airfoil used. Due to which, the drag polar can characterize an aircraft and the UAV in our case. Many performance parameters also depend on drag polar. The drag polar can be calculated with the following simplified equation where we assume that minimum drag occurs at zero lift.

Equation

$C_D = C_{D0} + KC_l^2$

Where the coefficient $K = \frac{1}{\pi ARe}$

AR= Aspect Ratio

e = Oswald efficiency factor

Using estimates based on [19] actual aircraft Oswald Efficiency factor for straight wing aircraft can be calculated as:

$e = 1.78(1 - 0.045AR^{0.68}) - 0.64$

$= 0.87$

K= 0.06

Coefficients for small UAV: $C_{D,0}$=0.0418

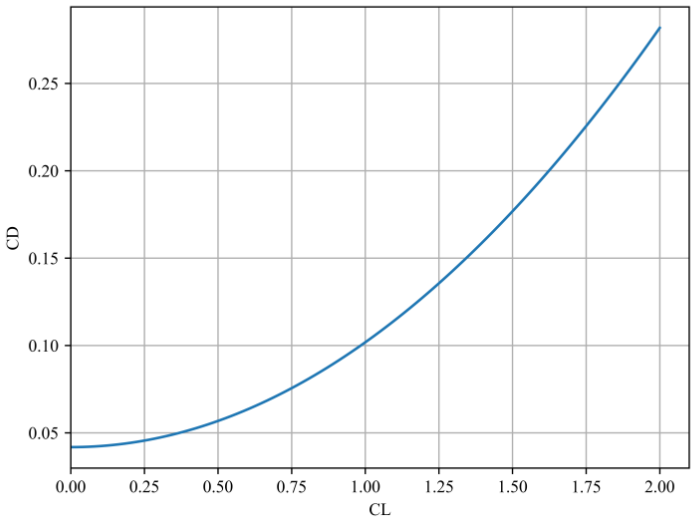

Figure 3. 6: Drag Polar

Thrust to weight ratio and Power to weight ratio

a) Using Thrust Matching:

In level unaccelerating flight, the thrust must be equal to the drag, whereas the weight must be equal to the lift

Thus, using this approach we can get T/W for cruise such that

$(T/W)_{cruise} = 1 / (L/D)_{cruise}$

$(T/W)_{cruise} = 0.08$

b) Thrust matching-II

In this approach, the thrust-to-weight ratio is driven by climb requirements.

$(T/W)_{climb} = (T/W)_{cruise}$ + Extra Thrust required for climb gradient

$(T/W)_{climb} = 1 / (L/D)_{climb} + V_{vertical} / V_{climb}$

$(L/D)_{climb}$ might be smaller than $(L/D)_{cruise}$ so we initially underestimate $(L/D)_{climb} = 10$

Where,

$V_{vertical}$ = Vertical velocity during climb: Requirement ≈ 3 m/s

V_{climb} = Horizontal velocity during climb

From FAR 25 requirement $V_{climb} > 1.2\ V_{stall}$

∴ $V_{climb} > 18$, say $V_{climb} = 20$ m/s

∴ $(T/W)_{climb} = 0.1 + 3/20$

$= 0.25$

b) Statistical estimation of T/W and Power Loading

T/W can be estimated from the historical data by using statistical power equations in the form of constant term times the independent variable to the power a constant term. i.e., $\alpha V^{c}_{max.}$ From the data given in [17] the values for α and c can be used as 0.005 and 0.57 respectively for homebuilt aircraft.

In case of our UAV, estimated maximum cruise speed V_{max} =18 m/s = 64.8 km/hr

Power to weight ratio (P/W_0)= αV^c_{max}

= 0.0539 watt/gram or kw/kg

= 5.5 watt/Newton

The equivalent thrust-to-weight ratio (T/W) can be calculated from the following equation:

$T/W = \eta_P/V * P/W$

Where propeller efficiency η_P =0.8

$T/W_0 = 0.8 / 18 * 5.5$

= 0.24

For initial layout, we select the highest value of T/W among the values obtained from preceding calculations. Thus the initial estimate for T/W is 0.25

Wing Loading

a) Stall Speed

The wing loading required to meet a certain stall speed requirement can be found by equating lift to weight.

$W=L=0.5\rho V^2_{stall} SC_{Lmax}$

$W/S = 0.5\rho V^2_{stall} C_{Lmax}$

Density of air at 1100 m altitude =1.08 kg/m^3

The 2D lift coefficient C_l for a plain wing with no flap can be estimated to be about 1.4. For low aspect ratio wings $C_{Lmax} \approx C_{lmax}$ = 1.4

$\therefore W/S = 170\ N/m^2 = 17.35\ kg/m^2$

b) Take-off distance

The total take-off distance is defined as the horizontal distance from the beginning of ground roll to the point at which the aircraft reaches an altitude of 50 ft. To find the required wing loading to meet a certain takeoff-distance requirement, a parameter can be obtained from figure 9 known as the take-off parameter (TOP) as provided in [25]

(W/S) = TOP $\sigma C_{L,T}$ (hp/W)

Where, σ = density of air with respect to sea level

$C_{L,T}$ = lift coefficient at take-off

(hp/w) = power to weight ratio in fps system = 0.099 hp/lb

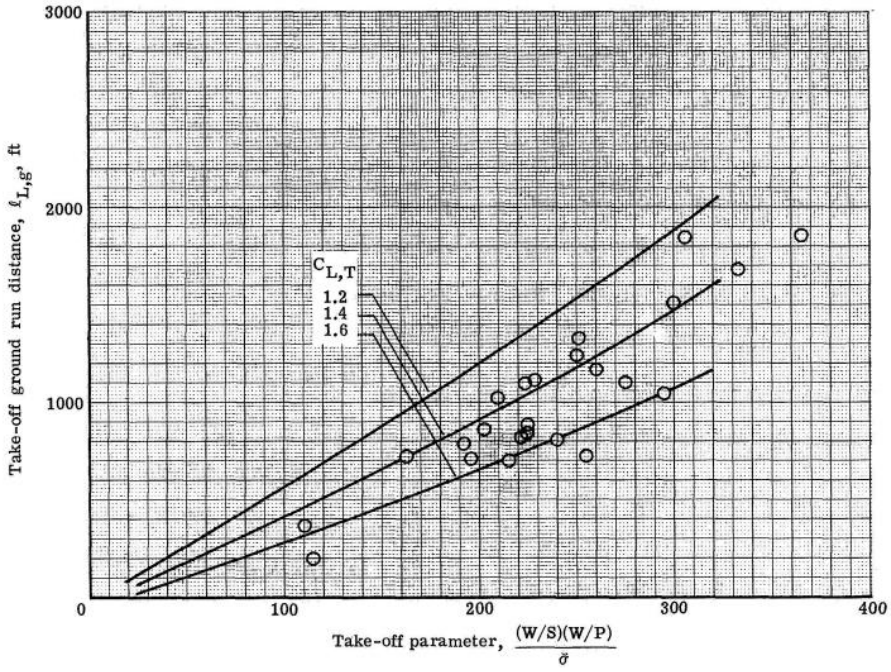

Figure 3. 7: Take off parameter vs. Landing Distance

Take-off speed is nearly equal to 1.1 times V_{stall} , $\Rightarrow C_{L,T} = C_{Lmax}/(1.1)^2 = 1.15$

For 196 feet ground run and $C_{L,T}$ =1.15~1.2, TOP ≈ 35

$\therefore$ (W/S) = 35 * (1.08/1.225) * 1.2 * 0.099

= 3.66 lb/ft^2

= 17.86 kg/m^2

The other method to find the design constraints for Take-Off conditions is given by [20] as:

$T/W = V_{TO}^{\ 2}/2g*SG + q_{T,O} C_{D,T} / (W/S) + \mu (1 - (q_{TO} C_{L,T}/W/S))$

V_{TO} =1.2 V_{stall} =18 m/s

SG= Ground Roll Distance= 50 m

G=9.81 m/s^2

q_{TO}=0.5 * 1.08 * 18^2 = 174.96

$C_{L,T}$=1.2

$C_{D,T}$=0.1

μ=ground friction coefficient = 0.03 for soft ground given by [21]

c) Rate of climb constraint and flight-envelope

Required rate of climb is 2 m/s.

V_{climb}=15 m/s

C_{DO}=0.0418

K=0.06

T/W = Rate of Climb/V_{climb} + (q_{climb} C_{DO})/(W/S) + k(W/S)/q_{climb}

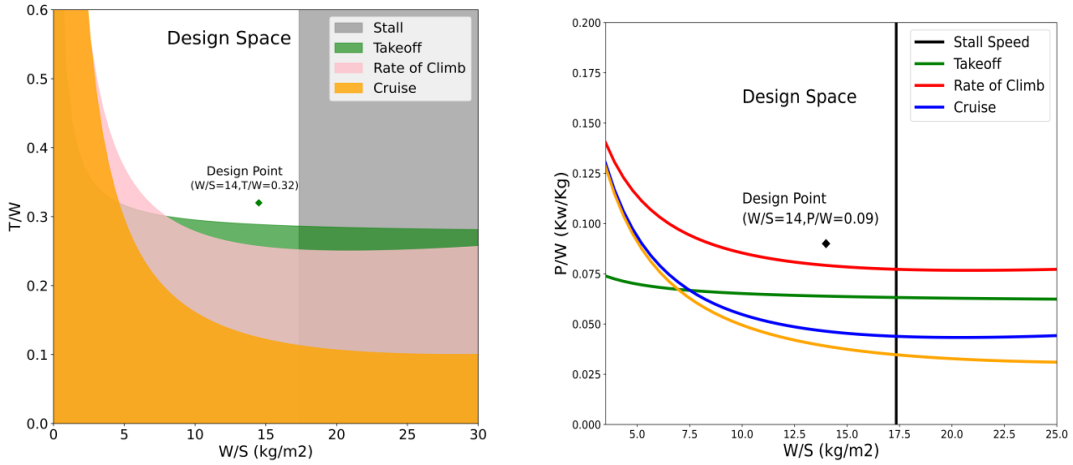

Figure 3. 8: Thrust to weight ratio vs Wing Loading (left) Power to weight ratio vs Wing Loading (right)

In the T/W vs. W/S diagram, we can find that the high thrust to weight ratio constraint has been imposed by the take-off requirement while in the P/W vs. W/S diagram the rate of climb parameter exceeds the P/W requirement for take-off conditions. It must be because one parameter could have higher thrust but lower power requirement than the other parameter in comparison.

3.2.4 Payload Description

The UAV is designed to hold the maximum payload of two kilograms. The payload is composed of medical commodities such as blood bags, vaccine vials and first-aid kit. The space to place the payload is allocated towards the front of the fuselage wherein an inclined platform is given for placement and ease of sliding the payload during the drop process. The width of the platform is 16 centimeters and the inclined length is 20 centimeters. The space for payload placement has a volume of 0.0024 m^3. For insulation, the payload compartment is covered with aluminum foil and foams are placed for shock absorption.

Figure 3. 9: Medical Payload

3.2.5 Payload Drop

The payload drop mechanism should be light weight, easy to manufacture and should be easily controlled by flight controller without using extra electronics. Some of the initial payload drop mechanism we designed are given below.

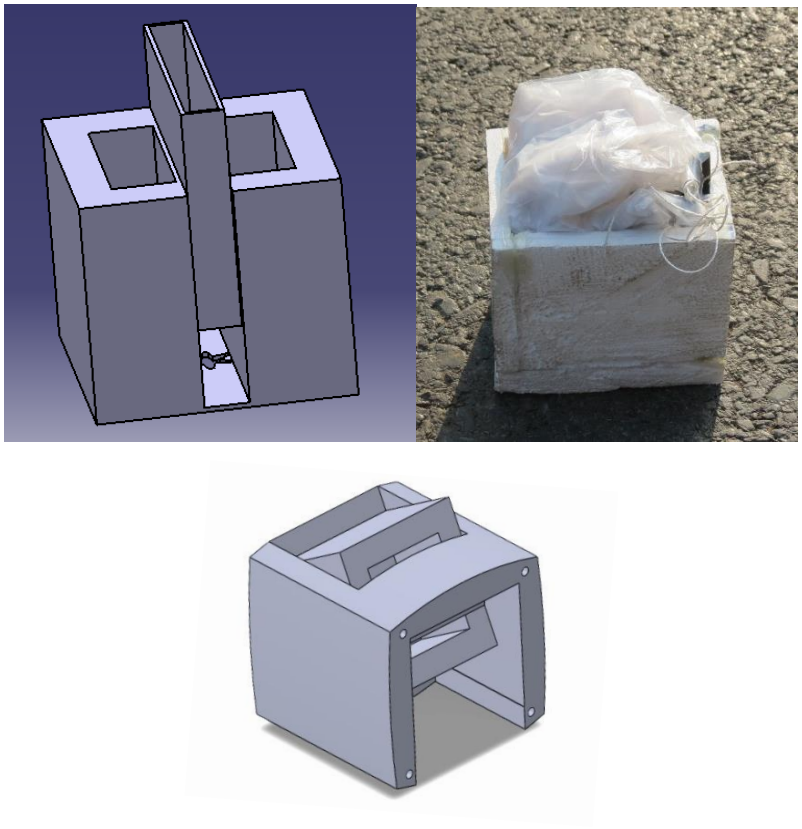

Figure 3. 10: Payload Compartment design options

Figure 3. 11: Payload Drop Access Panel

- After analyzing the different finally decided to use mechanism 1. We decided to use mechanism 1 because of the following reason.
- The door will not largely disturb the airflow and will not create much drag during operation

- Can operate with only one servo motor so easy to control by Flight Controller.
- Light weight and easy to manufacture.

3.2.6 Parachute

A parachute is a device used to slow the motion of an object through an atmosphere by creating drag (air resistance). Parachutes are usually made out of light, strong fabric, originally silk, now most commonly nylon.

Figure 3. 12: Parachute

A variety of loads are attached to parachutes, including people, food, equipment, space capsules, and bombs. Different shapes of parachutes like Hexagonal, Semispherical, Cross parachutes, paragliding etc. are practiced.

Size Calculation:

The size of the parachute is calculated using the following formula:

$$V_t = \sqrt{\frac{2m}{Cd.\rho.A}}$$

Where,

Vt = Descent velocity of the payload box

m = mass of the payload

Cd = Drag coefficient of the parachute

ρ = Density of the air (around 1.255 kg/m^3)

A = Total area of the parachute

Steps for making Parachute:

Step 1:

Get a square shape plastic of dimension 1m × 1m.

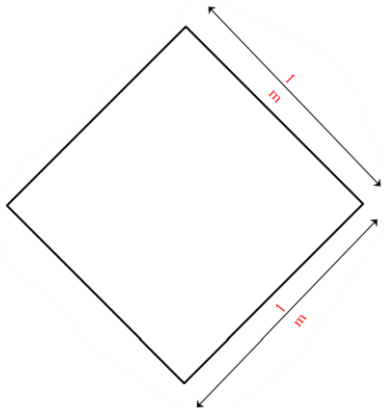

Figure 3. 13: Step 1

Step 2:

Fold in half diagonal.

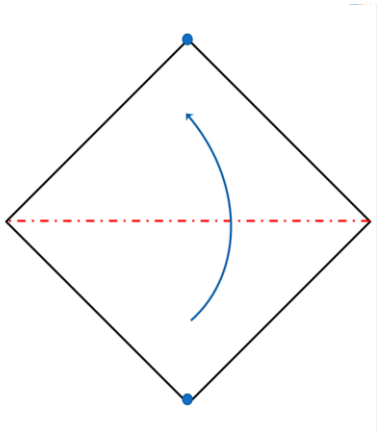

Figure 3. 14: Step 2

Step 3:

Mark the points somewhere above the two upper midpoints (Near to the midpoint).

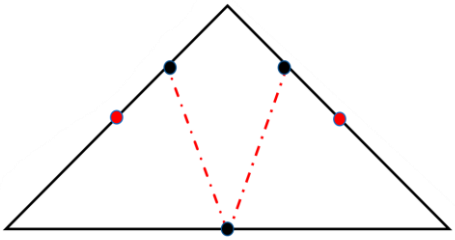

Figure 3. 15: Step 3

Step 4:

Fold diagonally into thirds making the red dotted lines as an axis.

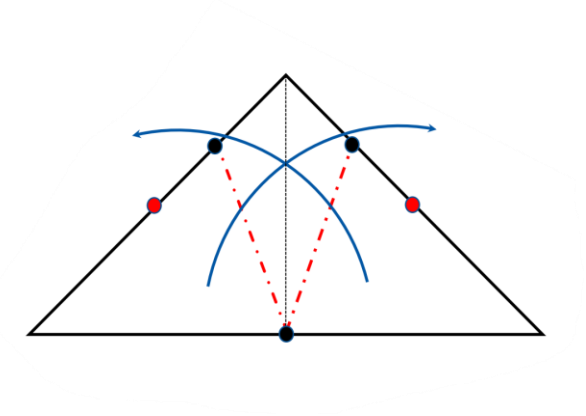

Figure 3. 16: Step 4

Step 5:

Maintain the symmetry and cut from the red dotted line.

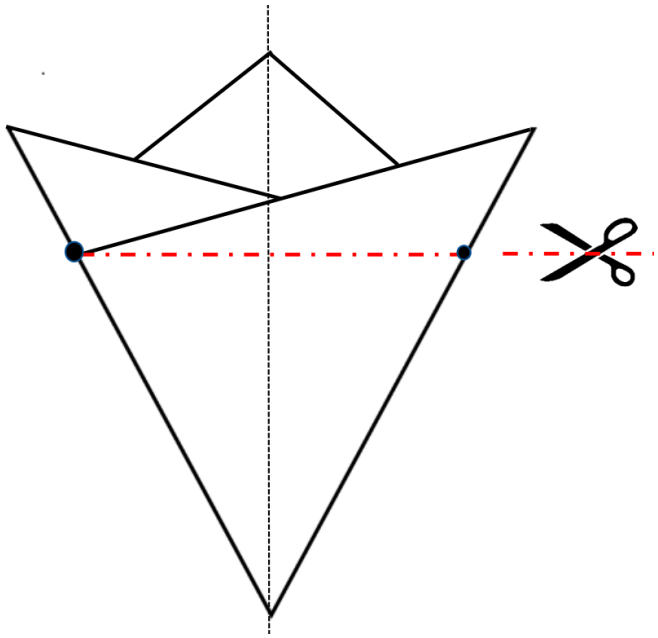

Figure 3. 17: Step 5

Step 6:

Get larger piece of the plastic and unfold it to get hexagonal geometry.

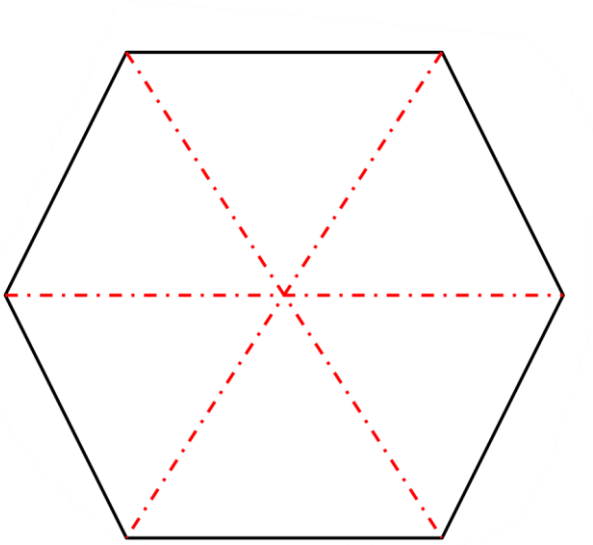

Figure 3. 18: Step 6

Step 7:

Stick cello tapes on each of the vertices of hexagon. Make holes of diameter of 2mm in each vertices. Insert the strings to each of these holes and tie them.

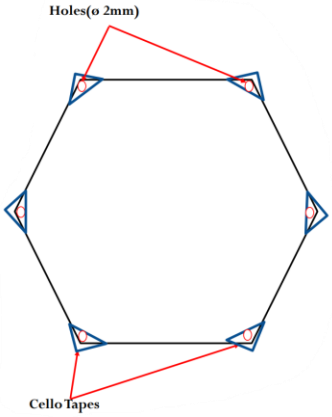

Figure 3. 19: Step 7

Eight nylon threads of length 1m were tied in the holes along the sides of the square plastic. Finally, all the threads were tied together and the threads were tied in the medical payload box.

3.2.7 Geometry Sizing

Wings

The wing of Aspect Ratio 7 is used without any taper or sweep. A dihedral of two degrees is used for lateral and directional stability. The actual wing size can be determined by dividing the gross take-off weight by take-off wing loading. Doing this, we get the reference area of the trapezoidal wing equal to 0.4 m^2. Now for aspect ratio of 7 the non-tapered wing span can be calculated as $b= \sqrt{(AR.S_W)} = 1.67$ m.

For span length of 1.67 m, wing chord (C_w) = S_W/b =0.23 m

Airfoil Selection

The airfoil to be used in wings was selected based on Weighted Scoring Method as provided in [28]

Seven different airfoils were considered for comparison of various criteria. For our UAV the important criteria are high range (high $(Cl/Cd)_{max}$), easy take-off(Cl_{max}), and high stall characteristics (high α_{stall}). The values of these parameters were obtained from Xflr5 for a Reynolds number of 300,000. The weight of the criteria is assigned accordingly as shown in the following table:

Table 3. 2: Airfoil Scoring Based On Various Criteria

Airfoil	**$C_L$max**	**α_{stall}**	**$C_{l,o}$**	**$(C_l/C_d)_{max}$**	**C_d min**	**C_m(c/4)**	**Weighted Score**
Weight	0.2	0.2	0.22	0.2	0.1	0.1	
NACA 2412	2.9	15	0.22	50	0.0065	-0.05	0.46
NACA 2415	2.2	15	0.22	45	0.007	-0.047	0.40
NACA 2418	1.6	16	0.22	40	0.0075	-0.045	0.36

NACA 4412	3.8	16	0.44	53	0.0068	-0.095	0.58
NACA 4415	2.3	16	0.38	43	0.0072	-0.077	0.45
NACA 4418	2.3	18	0.4	40	0.0077	-0.085	0.45
S9000	3.7	12	0.32	55	0.0061	-0.068	0.52

Comparison of weighted scores of a few airfoils from different series, NACA 4412 has the highest score based on the criteria mentioned above. Thus, NACA 4412 is selected as the airfoil to be used in the wings.

For airfoils used in horizontal and vertical tail, the criteria considered are low drag and good lift characteristics. Symmetric airfoils are used in tail as they are adaptable in both the upper and lower position of the tail section. NACA 0012 is widely used as tail airfoil as it possesses the features mentioned above. Moreover, NACA 0012 is easy to manufacture and it has been extensively tested and researched upon. So we select NACA 0012 as the airfoil to use in both the vertical and horizontal tail.

Fuselage

This UAV does not use a circular cross section for its fuselage. It rather has a filleted rectangular cross section in order to simplify the fabrication of payload compartment access panels and for allowing a larger space for the placement of the payload. The fuselage length can be initially estimated with the help of statistical equations provided in [17], which is based upon takeoff gross weight.

The statistical equation is Length= a W_0^c

For Homebuilt aircraft the values of a and c can be used as 1.28 and 0.23 respectively.

∴ Length of fuselage for take-off gross weight of 6 kilograms = 1.93 m

However, this is only a tentative calculation. The actual length of fuselage should depend on the moment arm required for longitudinal stability of the UAV. Hence, the length of

fuselage is calculated with the help of Xflr5 software by satisfying the necessary longitudinal stability criterion.

Another parameter, known as fuselage fineness ratio is calculated for identifying whether we have achieved the optimum fuselage design. Fuselage fineness ratio is simply the ratio of fuselage length and its maximum diameter or equivalent diameter. According to [22], the optimum fineness ratio for minimized drag is somewhere between 6 and 8.
For our UAV, The rectangular cross sectional area is 20 cm x 22 cm. The equivalent diameter is then calculated, which is equal to 0.23 m

∴ Fuselage fineness ratio = 1.93/0.23 = 8.93

The value is higher than the optimum requirement so the fuselage length is made shorter than the initial estimate. Using the fuselage length of 1.5 we get fineness ratio of 6.52 which falls under optimum value as suggested in [22]

Horizontal Tail

The size and location of horizontal tail has been determined by using the historical data for tail volume coefficient which is already used by most aircrafts with the similar configuration. The typical value for horizontal tail volume coefficient c_{HT} taken from [17] for homebuilt aircraft is 0.50 and that for vertical tail volume coefficient c_{VT} is 0.04.

$c_{HT} = L_{HT}S_{HT}/C_wS_w = 0.5$

and $c_{VT} = L_{VT}S_{VT}/b_wS_w = 0.04$

Using $L_{HT} = 1.2$ m

∴ $S_{HT} = C_wS_w\, c_{HT}/L_{HT} = 0.0448$

and $S_{VT} = b_wS_w\, c_{VT}/L_{VT} = 0.02$

For horizontal tail, low aspect ratio should be used for its effectiveness in high angle of attack or when the wing is already stalled. Using an aspect ratio of 3, we get the span of horizontal tail = 0.5 m. The corresponding chord length for horizontal tail is 15 cm.

Similarly, using half the aspect ratio of horizontal wing for vertical wing, the span is calculated as 0.18 m. The corresponding chord length for vertical tail is 15 cm. With fourteen degrees sweep, the span, the root chord and tip chord are 18 cm, 15 cm and 10 cm respectively

Propulsion System Specifications

For the ease of use and the off-shelf availability of components, electric engine is used in our UAV. The propulsion system consists of a LiPo battery with 6 cells in series, which provide 3.7 volts each. The battery drives a brushless motor with 650 KV rating, in which a 13" x 4" propeller is attached for thrust generation. The other details are provided in table 3.

Table 3. 3: Engine Specification

1.	**Battery Capacity**	**5000 mAh**
2.	Battery Voltage	22.2 V/ 6S1P
3.	Battery Weight	812 g
4.	Battery Size	56x51x146 mm
5.	Motor rating	650KV (650 rpm per volt)
6.	Motor Weight	131 grams
7.	Motor Maximum Thrust	2.8 Kg at 28.3 Amperes
8.	Motor Thrust at 10 Ampere load	1.43 Kg
9.	Motor RPM at 10 Ampere load	7810
10.	Battery Specific Energy	136 Wh/Kg

Power Analysis

A bench test using thrust stand was done to analyze power consumed to generate the required amount of thrust. The drop in voltage of the battery and the reduction in maximum thrust available at specific time can indicate whether the selected engine would provide the power necessary to carry out the mission.

The equation of climb is $(T-D)/W = \sin \gamma$

Where, γ is climb angle

Thrust required during climb $T = \gamma W/ + D$

The selected engine can only provide maximum thrust of 2.8 kg

So the UAV cannot climb at angle more than 20 degrees

For 20 degrees climb angle T = 2.8 kg

Thrust required for cruise

T = D = 7.55 N = 0.77 Kg

Thrust stand details

A 13x4 propeller was assembled with 650 KV brushless motor which was connected to a 6S, 3600 mAh LiPo Battery. It was fastened to a thrust stand and the amount of thrust as mentioned in the following table were provided for respective time period and the corresponding drop in voltage of the battery was noted as follows. The initial thrust available was calculated using the thrust relation provided by [27].

Table 3. 4: Power Analysis

Mission Phase	Time	Initial Battery Volts	Starting RPM	Initial Thrust Available (In Kgs)	Thrust Applied during Test	Final Battery Volts
Climb	60 seconds	25.1	16000	3.43	2.8 Kgs	23.8
Cruise	12 minutes	23.8	15400	3.03	1.1 Kgs	19.2

The result from bench test shows that with a 6S, 3600 mAh battery the flight is only possible till 12 minutes of the cruise with a cruise speed of 18 m/s. This will give a range of 12 kilometers. Similarly, at cruise speed of 15 m/s, a range of 16 kilometers can be achieved.

Energy of 6S 3.6 Ah battery = 90 Wh

We require a battery of double power to carry out the two-way flight. So the battery which can provide energy of at least 180 Wh should be used for this mission.

Landing Gear

Tricycle and Taildragger are the most widely used configuration for conventional landing gear system. To avoid hindrance to payload drop, it is better not to place landing gear too close behind the payload drop access panel, which is nearly at the longitudinal C.G. position. With this consideration, tricycle arrangement is not favorable to be used with our UAV. Taildragger, on the other hand provides benefits like higher propeller clearance for puller aircraft, and has less drag and weight than the tricycle landing gear. It also allows the wings to generate more lift for rough-field operations.

The landing gear has arrangements as shown in the figure below:

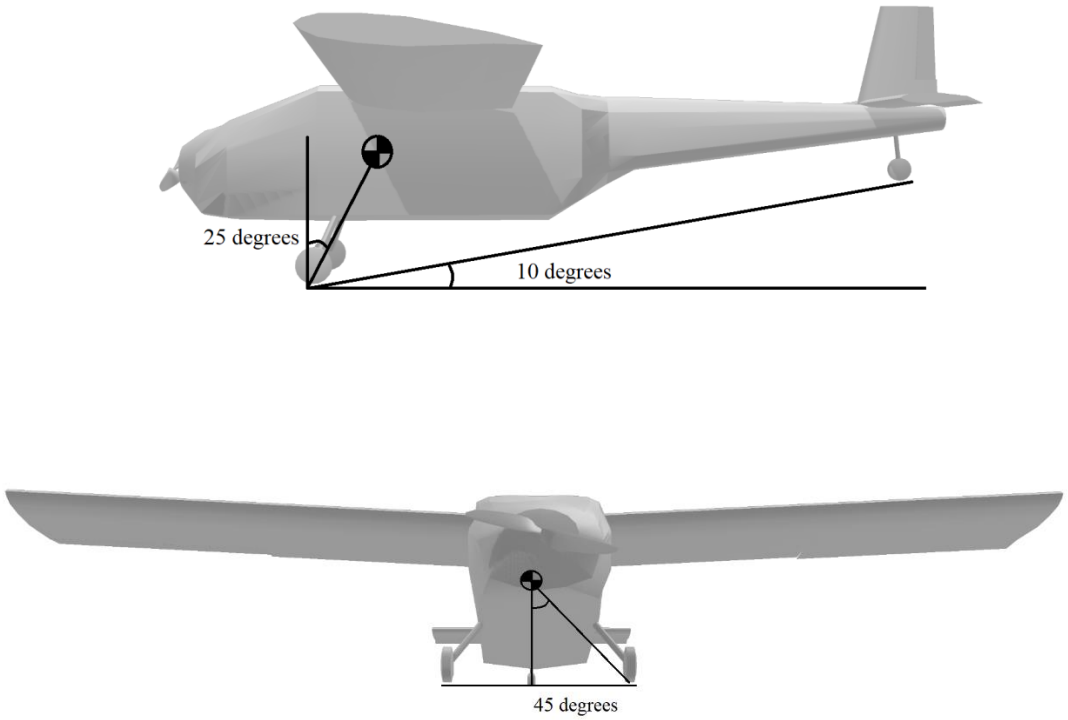

Figure 3. 20: Landing gear geometry and Locations

Final Layout

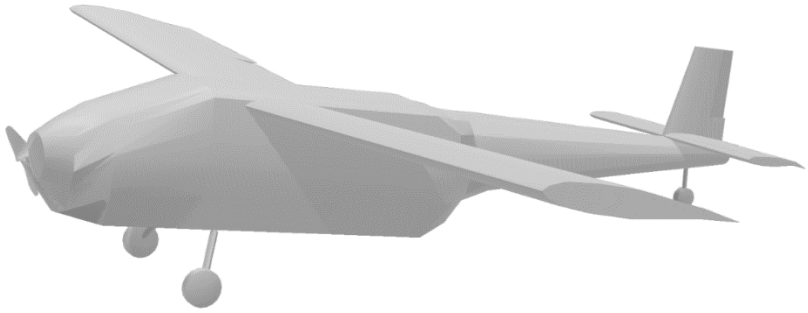

Figure 3. 21: Final Design of UAV

3.2.8 Performance Parameters

Endurance

The endurance of this UAV can be calculated based on the amount of power consumed by the electrical components to keep the UAV flying. From the propulsion system specifications provided above, we can find that the battery can provide electrical energy for a maximum of one hour if 5 ampere current is used continuously

The high power-to-weight ratio and the corresponding power consumption during the take-off and initial climb has been imposed only due to the take-off constraints. During these phases, the initial estimate of power loading can be used, i.e. 1.2 Kw/Kg. However, during the cruise only a fraction of maximum power available is necessary. In this phase, the power of about 0.4 horsepower is enough to fly the aircraft in constant velocity cruise of desired cruise velocity.

Level Flight Endurance or Loiter time (hrs):

$$E = 3.6 \frac{L}{D} \frac{E_{sb} \eta_{b2s} \eta_p}{gV} \frac{m_b}{m}$$

Where:

V= velocity (km/hr)

E_{sb} = battery specific energy (wh/kg)

η_b = propeller efficiency

The total system efficiency from battery to motor output shaft η_{b2s} is simply, the product of the efficiencies of the various components. Total battery to motor efficiency is therefore about 93%. [17]

Using the propeller efficiency of 0.8 and velocity of 90 km/hr, we get

Level Flight endurance = 0.58 hours = 34 minutes.

Range

The range for an electric aircraft can be found by multiplying flight time by velocity.

Level Flight Range (km):

$$R = 3.6 \frac{L}{D} \frac{E_{sb} \eta_{b2s} \eta_p}{g} \frac{m_b}{m}$$

∴ R = 34*60 seconds * 18 m/s = 36 km.

This value of range, however, cannot be achieved because the power consumed during take-off and climb is not considered. A thorough analysis of power consumed during climb has been performed using a thrust stand as mentioned in previous sections.

For climb mission segments, the vertical velocity or rate of climb can be calculated as follows:

$$V_v = \frac{1000\ \eta_P}{g} \left(\frac{P_{used}}{m} - \frac{V}{L/D} \right)$$

Where,

P_{used}/m = Power to weight ratio in (Kw/kg)

For our design power loading of 0.12 Kw/Kg, the rate of climb is then calculated as:

$\therefore$ $V_v = 3.4$ m/s.

This vertical velocity is excess from our required rate of climb i.e. 2 m/s because of the higher value of power-to-weight ratio imposed by the take-off requirement. For the phases other than take-off, a lower value of power can be used to achieve the required climb-rate. The propeller aircraft in level flight will have thrust equal to drag. So the power used during the cruise can be calculated with the following the relation

$$P_{used}\,\eta_p = \frac{mg}{(L/D)}V$$

$P_{used} = 153$ Watt

So the required power to weight ratio during the level flight is only 0.0225 Kw/Kg.

Take-off and Landing

The take-off ground roll can be calculated with various approximations and simplifications as mentioned in [24]. The simplified take-off ground roll s_g depending only on T/W, W/S and C_{Lmax} is as follows:

$$s_g \approx \frac{1.21\,(W/S)}{g\rho_\infty\,(C_L)_{max}(T/W)}$$

$s_g = 38$ m

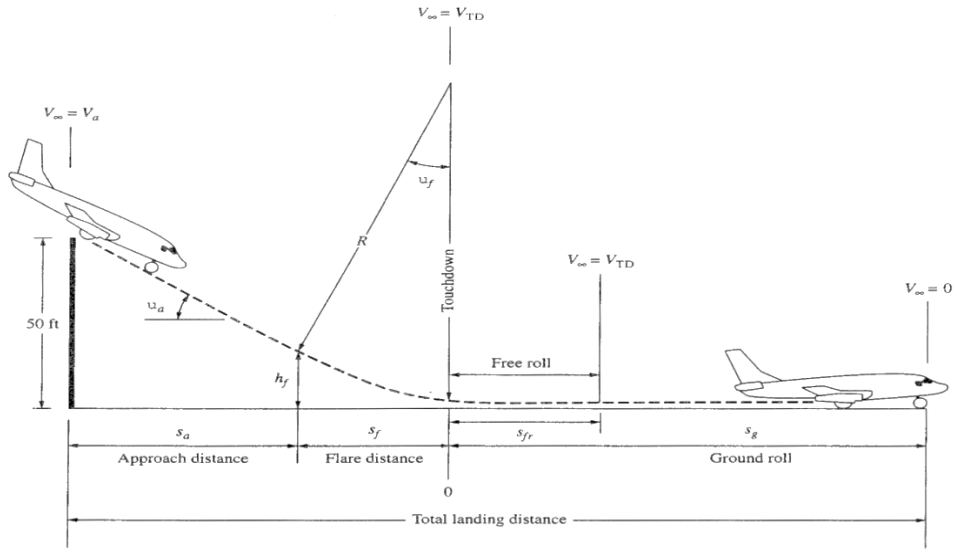

Figure 3. 22: Landing Phases [24]

Total landing distance is covered by the following phases:

Approach: The landing begins when the aircraft clears an obstacle height of 50 ft. At this instant, the aircraft follows a straight path with angle θ_a. The velocity of approach is required to be 1.3 V_{stall}.

In our case, the UAV should start approach at 30 degrees to flare at 10 feet above the ground, so the approach Distance s_a = (50- h_f) / Tan θ_a = 69 feet (21 m)

Flare: At a distance h_f from the ground, the aircraft transitions from the straight approach to ground roll. It can be considered that the flight path for flare is a circular arc with radius R, as shown in figure 25.

Flare distance we want flare distance to be no more than 30 feet s_f = R sin θ_a. So the radius of curvature of flare should be 60 feet (18m)

Ground Roll: When the wheels touch the ground, touchdown happens at the speed of V_{TD} = 1.15 $V_{stall.}$. After touchdown, the aircraft is in free roll before the brakes are applied. Ground roll distance is the distance from the touchdown to the point where the aircraft's velocity comes to zero.

The ground roll distance for landing is given by the following relation provided in [24]

$$s_g = jN\sqrt{\frac{2}{\rho_\infty}\frac{W}{S}\frac{1}{(C_L)_{\max}}} + \frac{j^2(W/S)}{g\rho_\infty(C_L)_{\max}\left[T_{\text{rev}}/W + D/W + \mu_r\,(1 - L/W)\right]_{0.7V_{TD}}}$$

Where, j = 1.15 for commercial airplanes

The value of coefficient of rolling friction μ_r can be obtained from the following data provided in [17]. We take μ_r= 0.2 for soft turf.

	μ_r(Typical Values)	
Surface	**Brakes off**	**Brakes on**
Dry concrete/asphalt	0.03–0.05	0.3–0.5
Wet concrete/asphalt	0.05	0.15–0.3
Icy concrete/asphalt	0.02	0.06–0.10
Hard turf	0.05	0.4
Firm dirt	0.04	0.3
Soft turf	0.07	0.2
Wet grass	0.08	0.2

Figure 3. 23: Friction Coefficient for different surfaces [17]

Consider free roll time of 3 seconds, no thrust reversal is applied so T_{rev} = 0

Then,

Stall speed = $\sqrt{\frac{2\,W}{\rho_\infty\, S\, C_{Lmax}}}$ = 13. 47 m/s

V_{TD} = 1.15 V_{stall} = 15.5 m/s

Assume C_L at ground roll = 0.1,

Lift at 0.7V_{TD} = 2.79 N

C_D= 0.0418 + 0.06 C_L^2 = 0.042

Drag at 0.7V_{TD} = 1.18 N

∴ s_g= 14.84 + 58.15 = 73 m

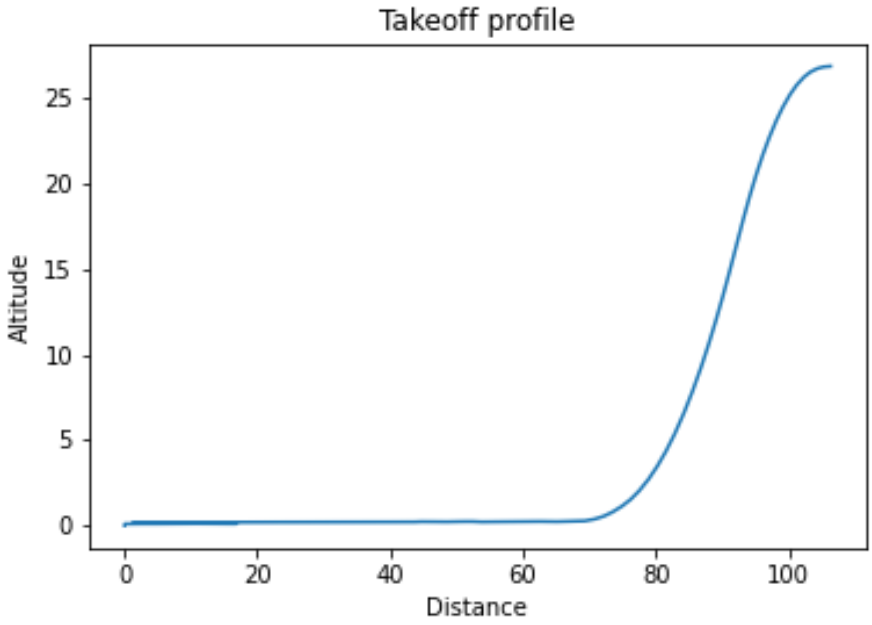

Figure 3. 24: Take off profile from flight simulation in Xplane

The takeoff profile was plotted by using the data obtained from X-Plane. The takeoff distance is 100m taking obstacle clearance distance of 25ft into account. The ground roll distance is 70m as shown in figure 27.

Center of gravity envelope

The location of center of gravity according to the design of our UAV is given in the following table.

X_{CG} **(metres)**	Y_{CG} **(metres)**	Z_{CG} **(metres)**
0.13	**-0.13**	**0**

Table 3. 5: Static Margin Shift

Allowable C.G travel ensuring longitudinal stability	**Static Margin (S.M.)**
Foremost Point (0.13 metres) Preferred location of C.G.	0.182
Aftermost Point (0.16 metres)	0.075 (41 % change)

3.3 Fabrication

3.3.1 UAS fabrication

The testing of payload drop mechanism was tested in our 1st prototype UAV. The existing UAV was modified to carry the payload and test the dropping mechanism. The same UAV was also used to check the functioning of Holybro PixHawk4 and its subsystem and did our first autonomous flight test.

Figure 3. 25: 1st Prototype UAV

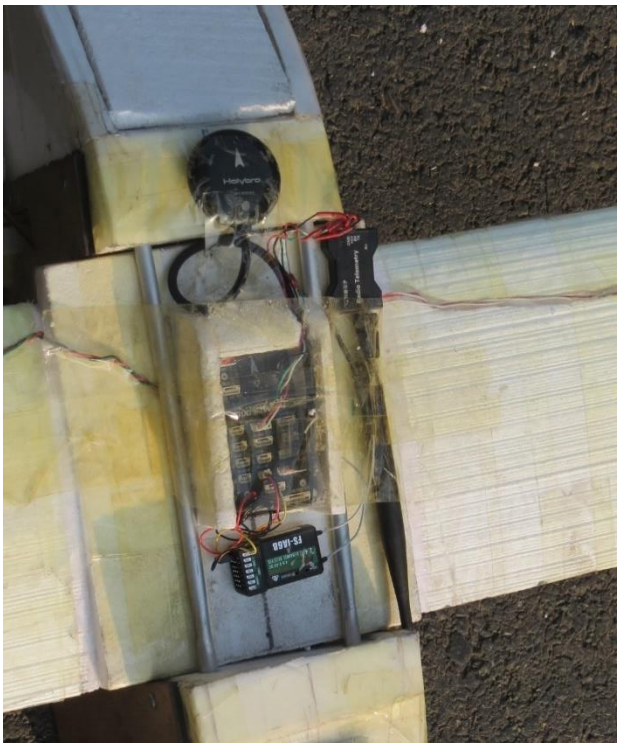

Figure 3. 26: Avionics

For our final prototype we made Wings, Empennage and most of the other parts out of Styrofoam. We used hotwire CNC machine to cut the foam in shapes of wings and fuselage wall. We used aluminum rods of 10 mm outer diameter and 1mm thickness as spars and used 9mm outer diameter with 0.5 mm thickness aluminum rods as longerons. We used the CNC LASER Cutter for plywood.

3.3.2 CAD Designs

All the laser cut and 3d printed parts were first designed in Catia V5. Most of the structural parts were made of the plywood which are lightweight and easy to work with. All the structural parts are designed in modular way so that if any crash happens it is easier to repair. All the plywood parts are joined together by dendrite.

3.3.2.1 Fuselage Design

Figure 3. 27: Fuselage frames and longerons

The frames are made of 3mm and 5mm thickness plywood. The front and rear frames are of 5mm plywood as they are the responsible for carrying loads during landing and the middle are of 3 mm thickness plywood as they are there only for support.

The 4 outer longerons are of 9 mm outer diameter and 0.5 mm thick aluminum rods. The middle longerons are of 10mm outer and 1mm thick aluminum rods. They are extended and bend from front frame to hold motor mount.

The motor mount is made of 8mm thick plywood to withstand the force from the thrust from motor.

3.3.2.2 Fuselage Skin

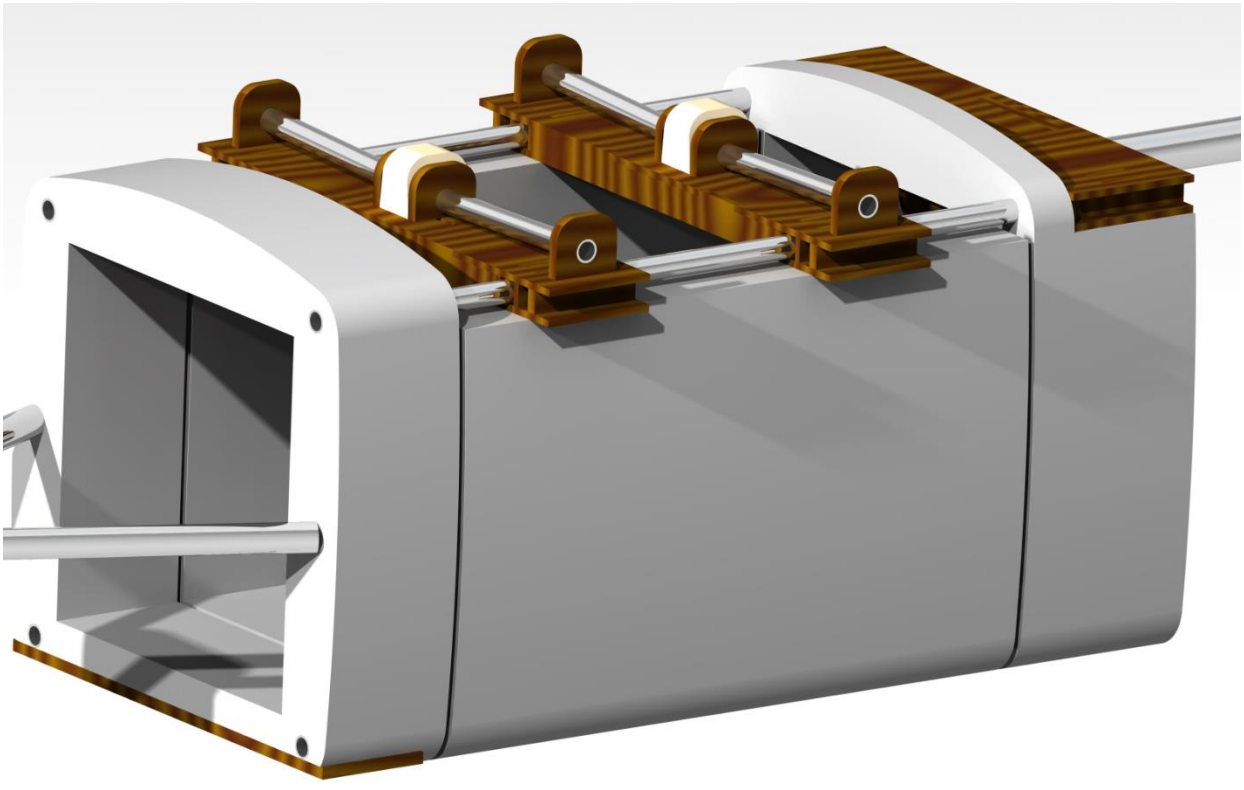

Figure 3. 28: Fuselage skin

The skin of fuselage is made of Styrofoam which resists the compression forces acting on

Figure 3. 30: Empennage Connection to Fuselage

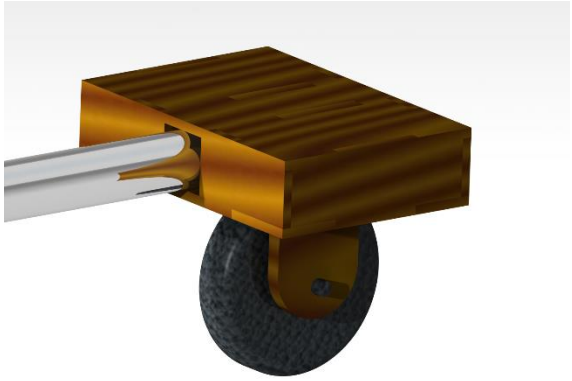

Figure 3. 29: Empennage Connection to Boom

it. The Styrofoam also acts as heat insulator for our medical payload. The foam are cut in pieces with the help of hotwire and assembled with longerons. Empennage Connection to

The empennage is connected to fuselage with the help of single 19 mm outer diameter 0.5mm thick aluminum boom.3 boom holder plywood is of 5 mm. They can be easily replaced in case of crash.

The empennage is glued to the plywood. This connection also acts as a housing for tail wheel.

3.3.2.3 Wing Mount Design

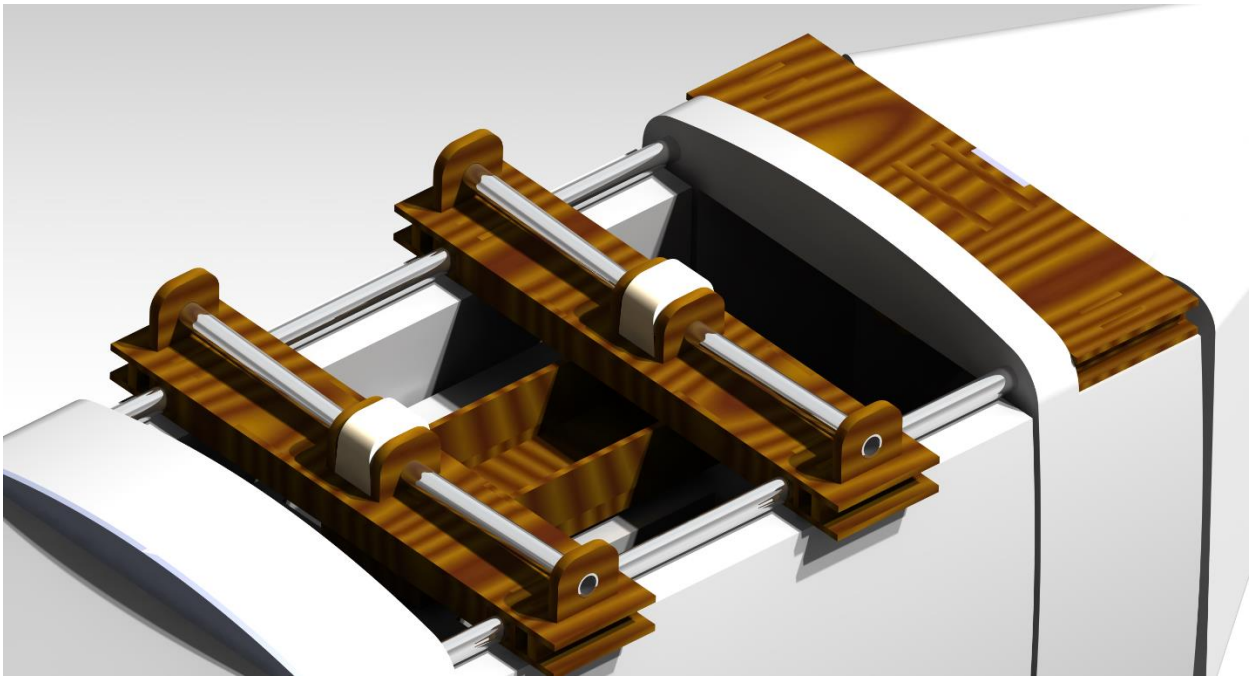

Figure 3. 31: Wing and Fuselage Connection

The wing is connected to fuselage through the aluminum longerons of fuselage.

We used 2 spar mount of 5mm ply which were cut to give 5 degree dihedral. All the others plywood except main load bearing part are made of 3 mm ply to reduce weight.

The aluminum rods are of 11 mm outer diameter and 10mm inner diameter . The rods of wing spar are of 10mm diameter which fits tightly and hence provide the additional support.

The connection of two spar is secured by part printed using TPU. The TPU is flexible which can absorb the loads from the wing.

3.3.2.4 Payload Section Design

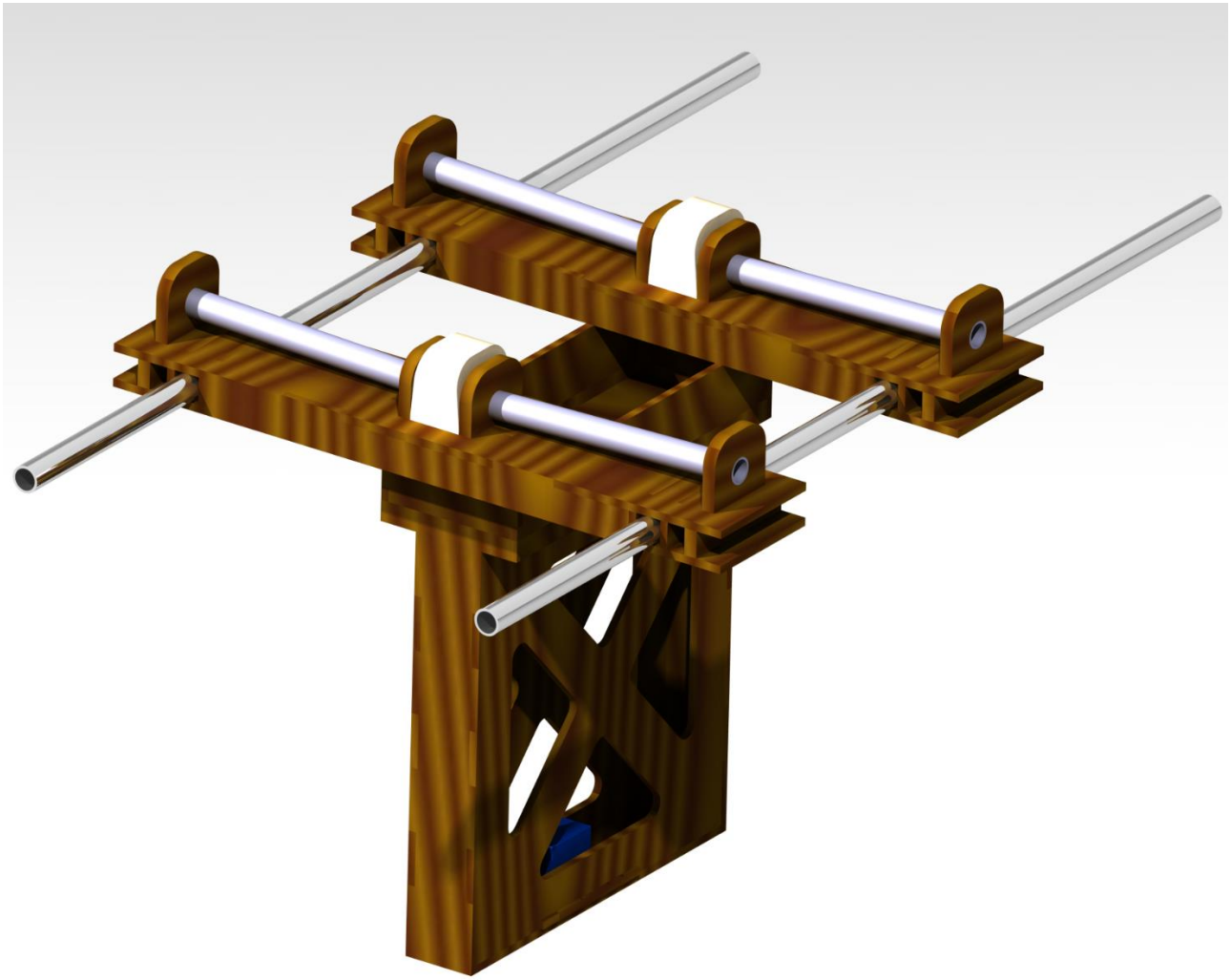

Figure 3. 32: Payload Section

The payload is supported by servo horn and the servo is held by above design.

The avionics bay is located between the two spar of wing which helped us to place the flight controller in the centroid of the plane which is essential for the operation of flight controller.

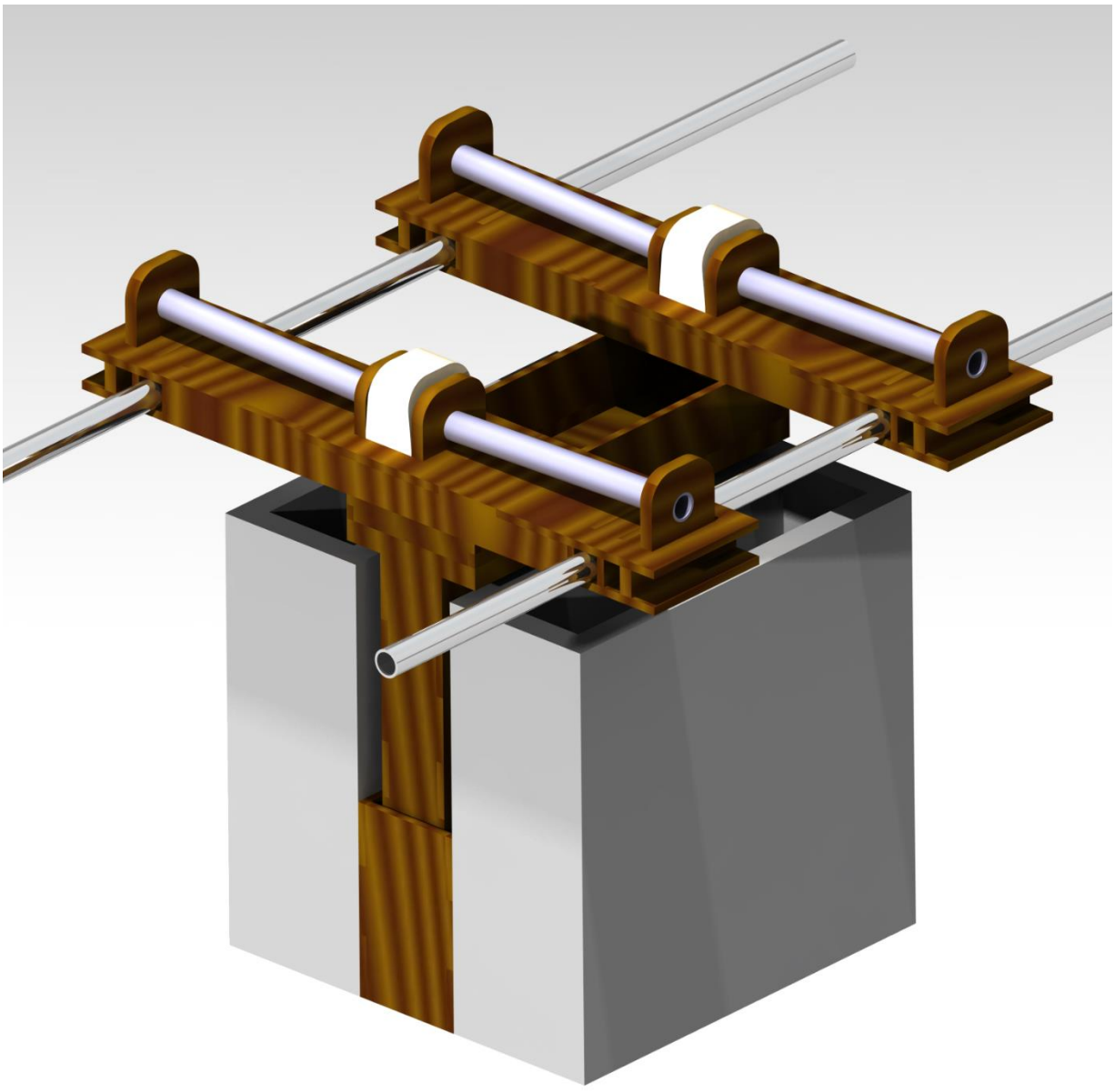

Figure 3. 33: Payload location and position

The payload is located in the centroid of the UAV so when dropped it doesn’t affect the stability.

Landing Gear

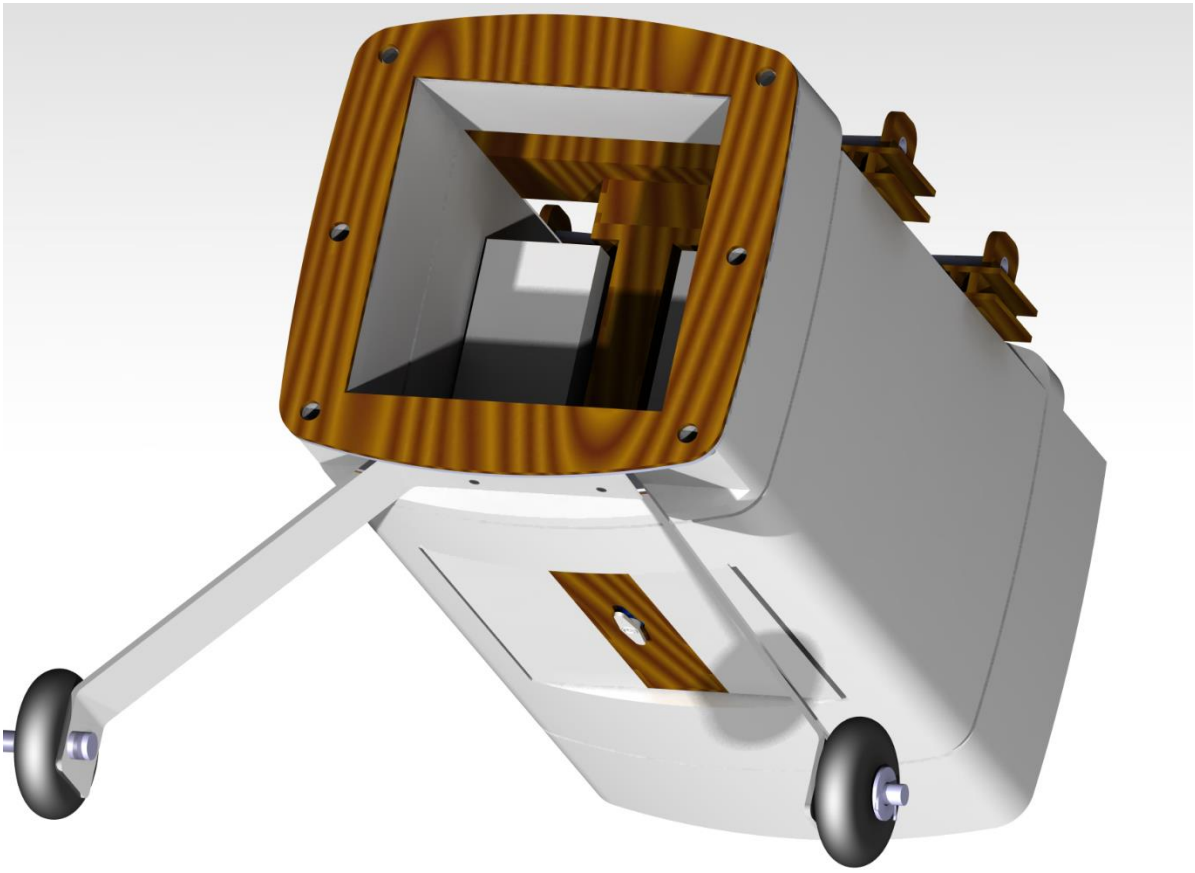

Figure 3. 34: Landing Gear

The landing gear is made using aluminum slab of thickness 3mm and Styrofoam wheels of diameter 14cm.

The landing gear is attached to the fuselage using 5 screws.

3.3.2.5 Insulation Cargo Container: Fabrication and installation

The main walls of the insulation container is made of expanded polystyrene. The walls is lined with aluminum to alleviate the emissivity of heat through the container walls. Medical goods will be wrapped with bubble wrap or similar shock absorbing material. The container is as airtight as possible so that heat emission to and from.

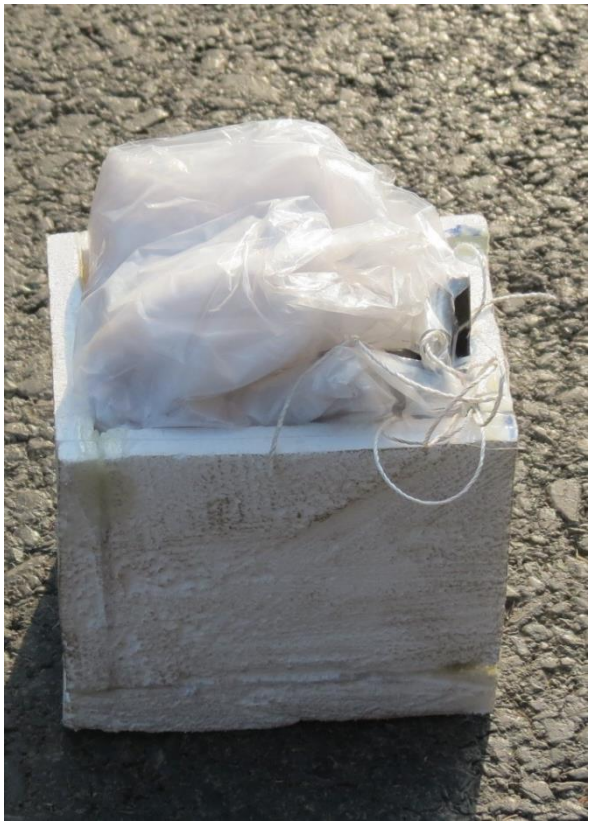

Figure 3. 36: 1st Prototype Payload box

Figure 3. 35: Final Prototype Payload box

The payload box if fitted with parachute. The combination of parachute and styrofoam will reduce the impact on payload while dropping from the UAV. The styrofoam box and aluminum lining will prevent the payload from surrounding factors such as humidity, temperature.

CHAPTER FOUR: RESULTS AND DISCUSSION

4.1 Results

4.1.1 Stability

The static and dynamic stability were computed using xflr5 software. For generating stability derivatives xflr5 treats wings as thin surface and solves using vortex lattice method (VLM). In this method, all the viscous effects are neglected and the flow field is assumed to be inviscid, incompressible and irrotational. During solution, the lifting surfaces are divided into number of panels and a ring vortex is placed on each panel. A Neumann boundary condition is applied at each control point (usually ¾ chord position) to obtain the following solutions:

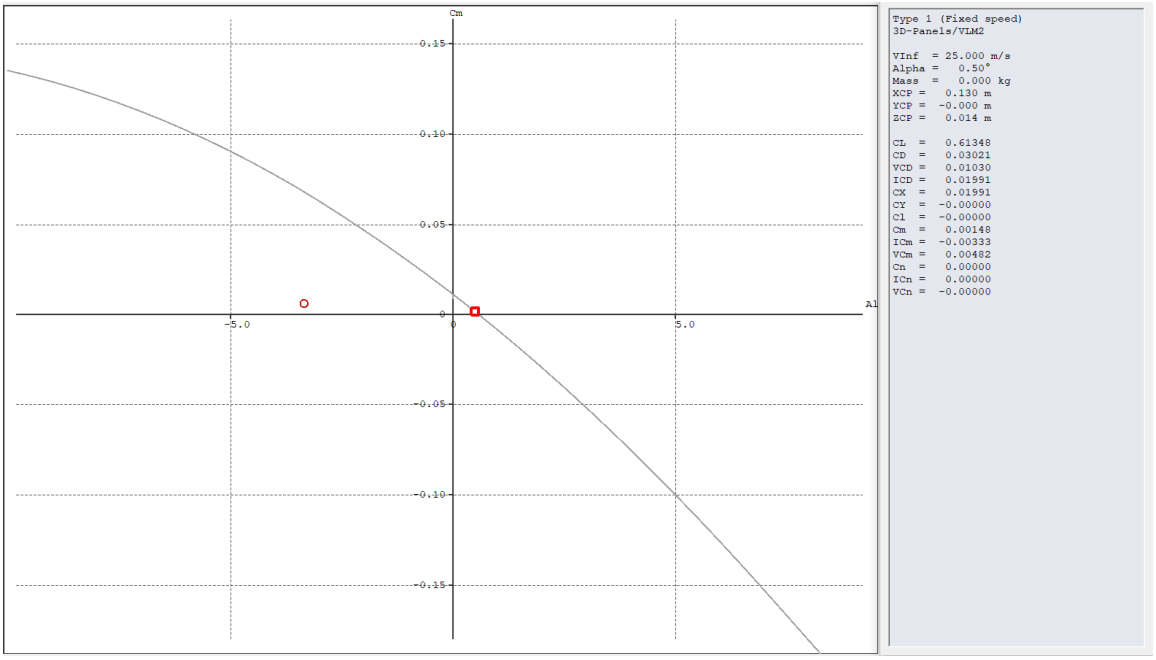

Figure 4. 1: Cm vs Alpha Curve from Xflr5

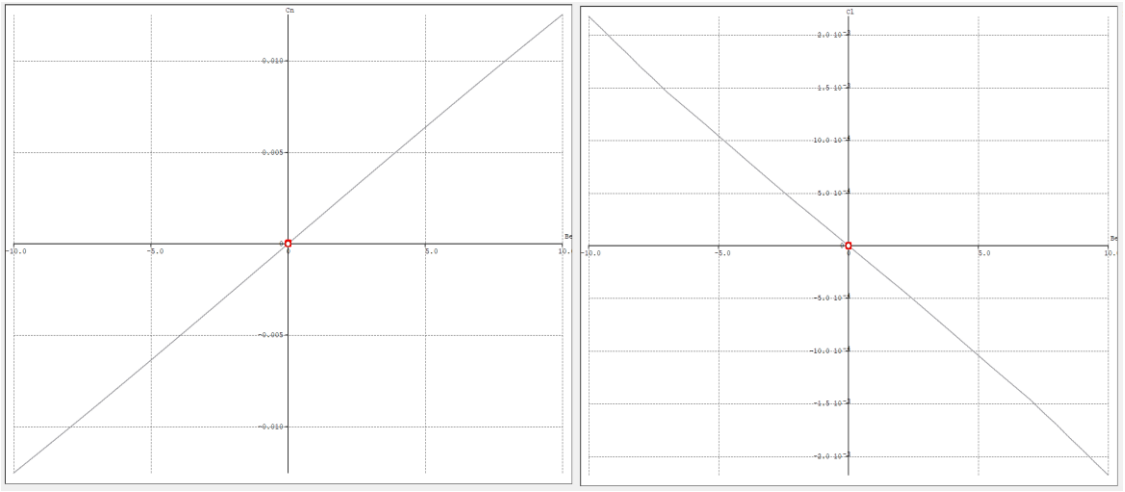

Figure 4. 2: Cn vs Beta (left) and Cl vs Beta (right)

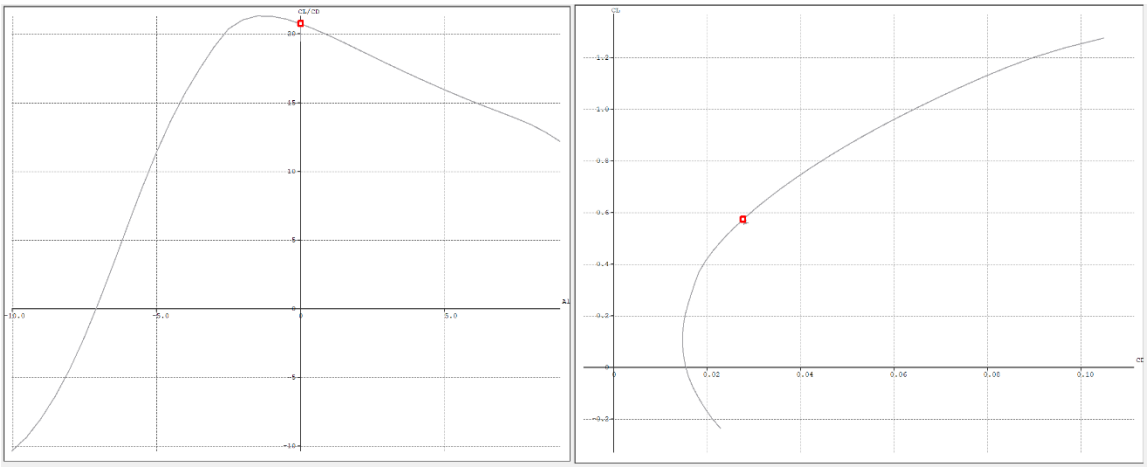

Figure 4. 3: CL/CD vs Alpha (left) and CL vs. Cd (right)

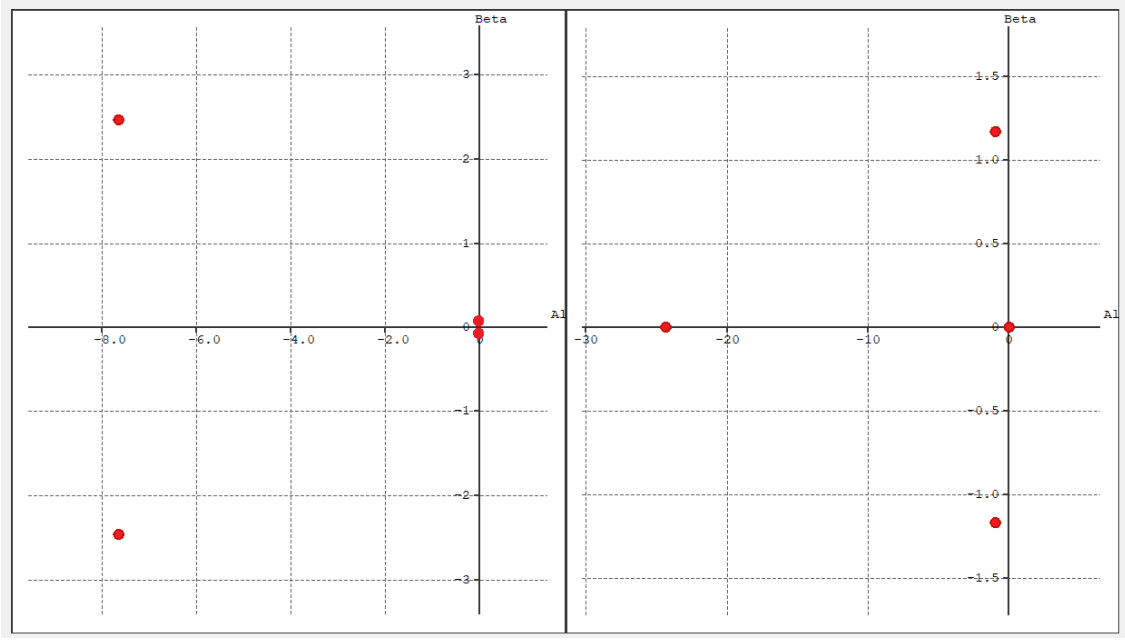

Longitudinal Modes

Directional and Lateral Modes

Figure 4. 4: Root of longitudinal mode (left) and lateral & directional modes (right)

Longitudinal Stability

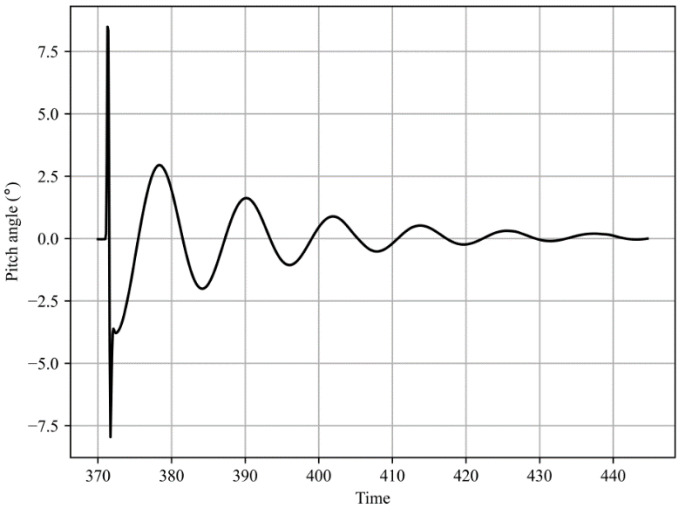

Figure 4. 5: Short Period Mode

Short period damping ratio $\zeta = 0.134$

Frequency = 0.08 Hz

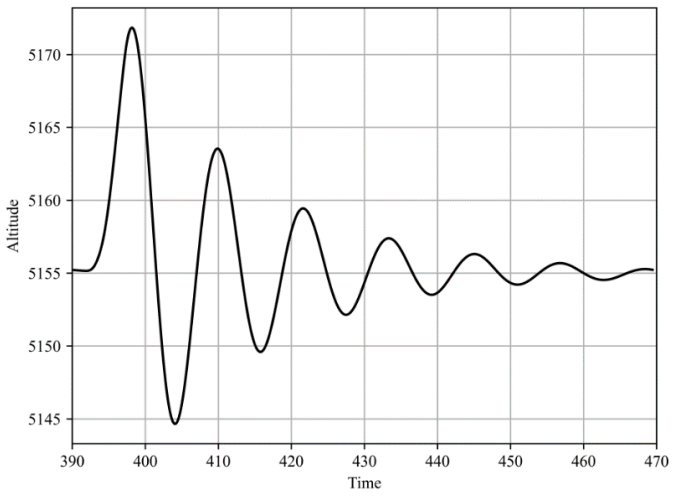

Figure 4. 6: Phugoid Mode

Phugoid mode damping ratio $\zeta = 0.084$

Frequency = 0.08

Directional and lateral stability

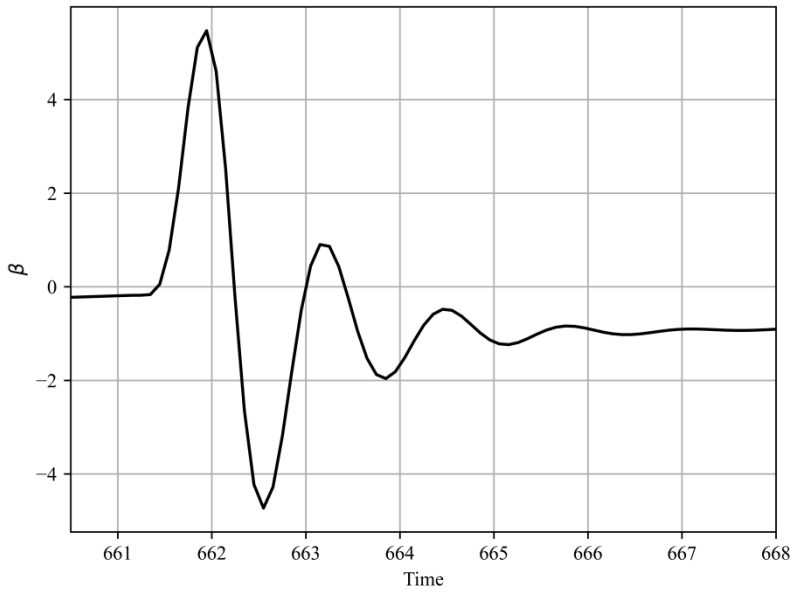

Figure 4. 7: Dutch Roll mode

Dutch roll damping ratio $\zeta = 0.25$

Frequency = 0.76 Hz.

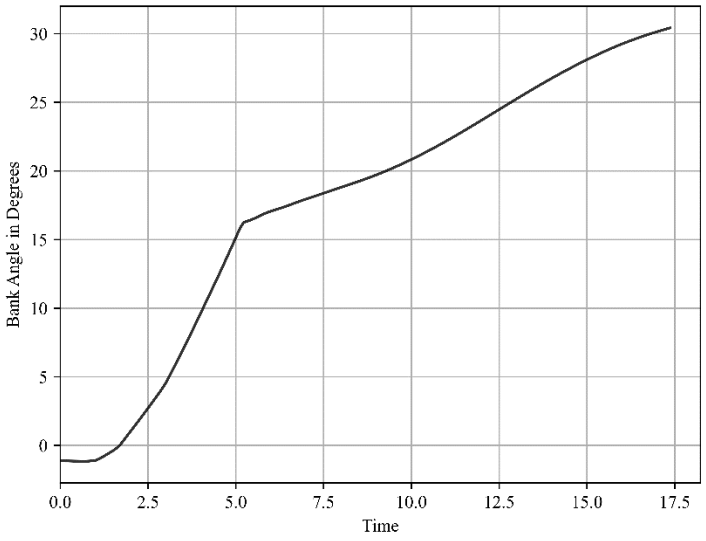

Figure 4. 8: Spiral Mode

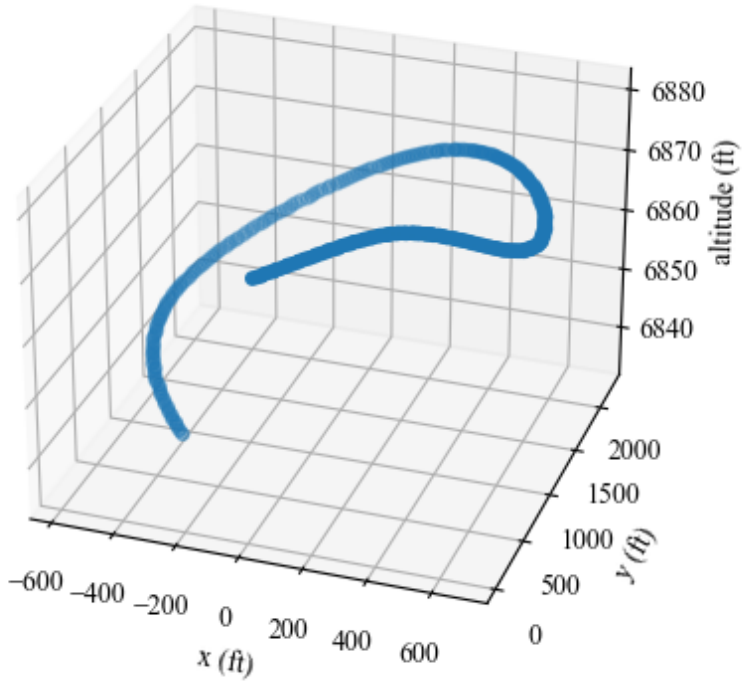

Figure 4. 9: 3D spiral path

4.1.2 Calculating the control derivatives

A longitudinal dynamics model can be obtained from Xlfr5 stability analysis.

State matrices

Longitudinal state matrix

$$\begin{pmatrix} \dot{u} \\ \dot{w} \\ \dot{q} \\ \dot{\theta} \end{pmatrix} = \begin{pmatrix} -0.0366361 & 0.258976 & 0 & -9.81 \\ -0.767013 & -5.8739 & 24.2408 & 0 \\ -0.0524602 & -9.9794 & -10.3861 & 0 \\ 0 & 0 & 1 & 0 \end{pmatrix} \begin{pmatrix} u \\ w \\ q \\ \theta \end{pmatrix} + \begin{pmatrix} -0.3831859 \\ 17.36877 \\ 248.4768 \\ 0 \end{pmatrix} \delta e$$

Where the state variables ($u\ w\ q\ \theta\ h$) refer to the longitudinal velocities (u and w), the pitch rate (q) and the angle of inclination (θ). The control input δe is the elevator deflection angle δe. Other control parameters like throttle settings could not be incorporated in the state matrix because it was not available in Xflr5.

Lateral state matrix

$$\begin{pmatrix} \dot{\beta} \\ \dot{p} \\ \dot{r} \\ \dot{\phi} \end{pmatrix} = \begin{pmatrix} -0.184623 & -0.0612912 & -25.52330 & 9.81 \\ -2.06564 & -26.4465 & 5.60273 & 0 \\ 1.63506 & -5.23653 & -1.13875 & 0 \\ 0 & 1 & 0 & 0 \end{pmatrix} \begin{pmatrix} \beta \\ p \\ r \\ \phi \end{pmatrix}$$

Where, β is the sideslip angle, p and r the roll and yaw rates and ϕ the roll angle.

4.1.3 Longitudinal modes

Eigenvalue:

-8.133+ -15.39i | -8.133+ 15.39i | -0.01503+ -0.4875i | -0.01503+ 0.4875i

---

Eigenvector:

1+ 0i | 1+ 0i | 1+ 0i | 1+ 0i

118.4+ 13.18i | 118.4+ -13.18i | -0.03052+0.0004379i | -0.03052+-0.0004379i

-2.636+ -76.39i | -2.636+ 76.39i | 0.02427+0.0007196i | 0.02427+-0.0007196i

3.951+ 1.917i | 3.951+ -1.917i | -0.003008+ 0.0497i | -0.003008+ -0.0497i

4.1.4 Lateral modes

Eigenvalue:

-25.78+ 0i | -1.019+ -7.342i | -1.019+ 7.342i | 0.04715+ 0i

Eigenvector:

1+ 0i | 1+ 0i | 1+ 0i | 1+ 0i

4.652+ 0i | -0.08518+ 0.03774i | -0.08518+ -0.03774i | 0.1105+ 0i

0.9223+ 0i | 0.03155+ 0.2829i | 0.03155+ -0.2829i | 0.891+ 0i

-0.1805+ 0i | -0.003465+ -0.01208i | -0.003465+ 0.01208i | 2.342+ 0i

4.1.5 Circuit diagram

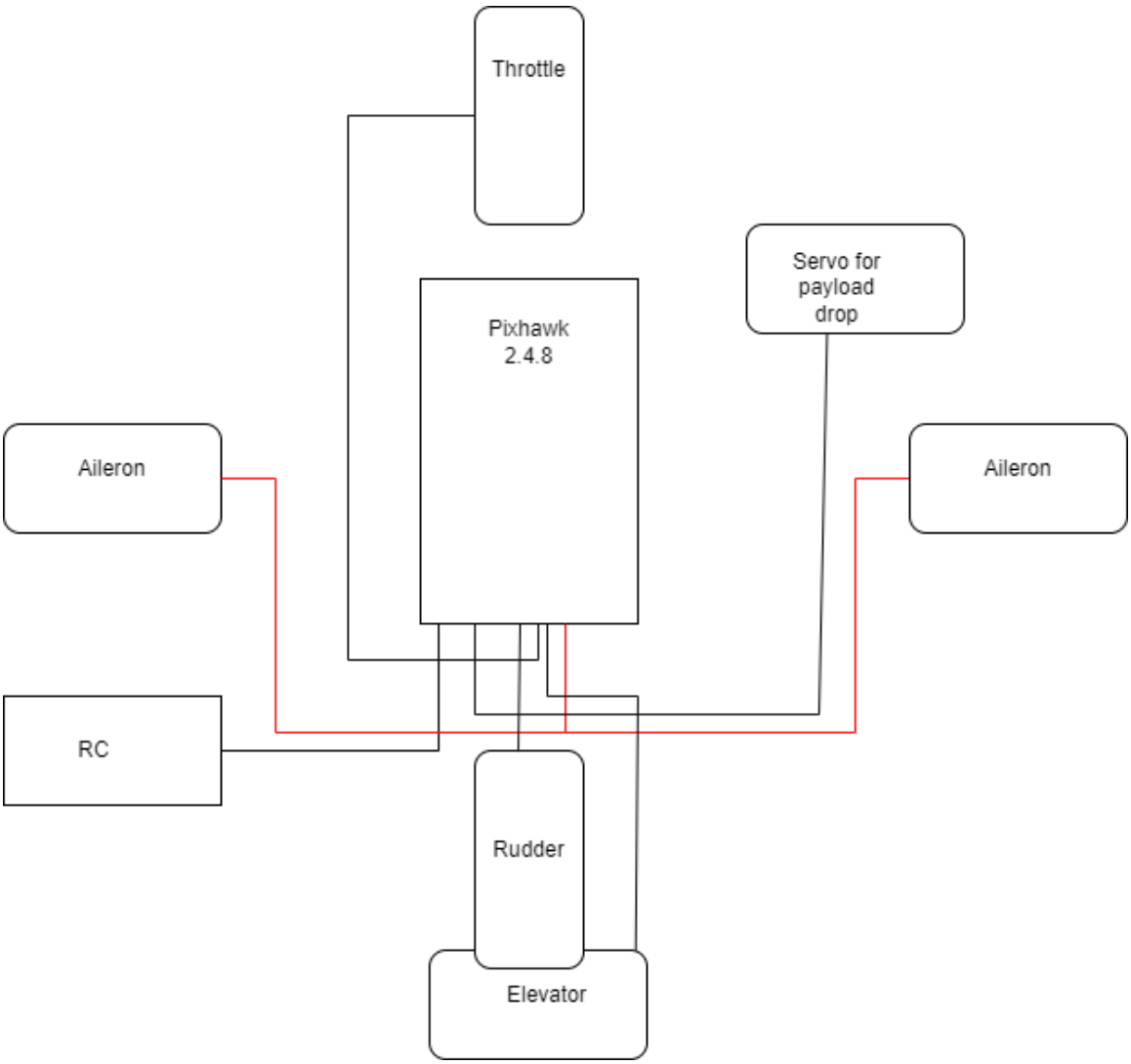

Figure 4. 10: Circuit diagram

4.1.6 Mission flight

The Unmanned Aerial Vehicle (UAV) was successfully tested in autonomous mode using Mission Planner. The tests were conducted in a controlled outdoor environment with a clear line of sight between the ground station and the UAV.

During the tests, the UAV was programmed to follow a pre-defined flight path, which included a series of waypoints and altitude changes. The UAV successfully completed the flight path as planned, without any manual intervention required.

In addition to following the pre-defined flight path, the UAV was also able to perform various autonomous functions, such as takeoff and landing, and return to home in case of communication loss with the ground station.

The performance of the UAV in autonomous mode was evaluated based on its accuracy in following the pre-defined flight path and its ability to respond to changing environmental conditions. The UAV was able to accurately follow the flight path within a reasonable margin of error, even in windy conditions.

DO_SET_SERVO command was set for the waypoint where payload was to be dropped.

Overall, the successful testing of the UAV in autonomous mode using Mission Planner demonstrates its capability to perform complex aerial missions with minimal human intervention.

Figure 4. 11: Typical Mission profile

4.2 Problems faced

- The command DO_SET_SERVO feature on QGroundControl ground station didn't work so shifting to mission planner was the only option.
- Due to lack of
- Due to lack of materials such as carbon fiber, balsa wood in the market, the zero fuel weight of UAV was increased .
- Due to lack of runway, during takeoff obtaining directional control was difficult.

4.3 Budget Analysis

The overall budget of the project can be illustrated in the tabular form.

Table 4. 1: Budget analysis

S.N.	Name of Product	Quantity	Rate	Total
1	Pix-Hawk 4 and it's accessories	1	60,000	60,000
2.	Radio transmitter and receiver	1	10,000	10,000
3	Brushless motors	2	8,000	16,000
4	Propellers	2	5,000	10,000
5	Battery	1	15,000	15,000
6	Servos	5	1,000	5,000
7	Electronic speed controller	1	5,000	5,000
8	Battery Charger	1	5,000	5,000
9	Tapes and Adhesives	NA		5,000
10	Documentation cost	NA		1,000
11	Miscellaneous	NA		5,000
			GRAND TOTAL	1,37,000

CHAPTER FIVE: CONCLUSION AND RECOMMENDATION

5.1 Conclusion

In conclusion, the design of a UAV using Xflr5 software has been successfully completed and has undergone several tests to ensure its stability and functionality. The results of these tests have shown that the plane is longitudinally stable and has a CG range that can travel from 13 cm to 16 cm behind the reference line. The optimal position for the payload is at the default CG position of 13 cm for stable flight. To avoid hindrances to payload drop and to the propeller, the taildragger configuration was selected. The payload compartment was successfully designed and tested with the deployment of a parachute. The bench test performed for practical analysis of power with a 6S 3600 mAh battery suggests that to complete this specific mission, a battery with energy of at least 180 Wh should be used.

In order to improve the design further, future works will include a detailed analysis and improvement in the structural design to handle aerodynamic and inertial loads. This will be followed by testing and the inclusion of detailed flight test data, such as best angle of climb, best rate of climb, and the flight envelope using the structural data. The autopilot has been successfully set up and tested with the UAV. However, the setup could not be made with QGround Control environment so we had to shift to Mission Planner software to set the servo command. The stability derivatives generated from the Xflr5 include assumptions that are not likely to be true in the real situation. So the actual flight test data and the corresponding value of the stability derivatives should be incorporated to generate a reliable flight dynamics model.

Overall, the design of the plane has shown promising results and the future works will further refine the design and improve its performance. The results of this study will serve as a foundation for future projects and provide valuable insights for the design of future UAVs. The successful completion of this project demonstrates the potential for the use of Xflr5 in the design of efficient and stable UAVs for various applications.

5.2 Recommendation

After completing the project following recommendations are made for design and fabrication of medical UAS.

1. Study and collection of terrain data of health posts of Nepal and path optimization software for delivery can be made.
2. Most of the crashes were faced during takeoff and landing. So, catapult takeoff and arrested landing can be implemented.
3. Wing and fuselage manufacturing techniques can be improved to reduce weight.

REFERENCES

[1] Rosser, J. J. C., Vignesh, V., Terwilliger, B. A., & Parker, B. C. (2018). Surgical and medical applications of drones: A comprehensive review. JSLS : Journal of the Society of Laparoendoscopic Surgeons, 22(3) https://doi.org/10.4293/JSLS.2018.00018

[2] Xu, Q., Ng, J. S. L., Tan, O. Y., & Huang, Z. (2014). Needs and attitudes of Singaporeans towards home service robots: A multi-generational perspective. Universal Access in the Information Society, 14(4), 477–486. https://doi.org/10.1007/s10209-014-0355-2

[3] Amukele, T., Ness, P. M., Tobian, A. A. R., Boyd, J., & Street, J. (2016). Drone transportation of blood products. Transfusion, 57(3), 582–588. https://doi.org/10.1111/trf.13900

[4] Austin, R. (2010). Unmanned aircraft systems. John Wiley & Sons, Ltd. http://dx.doi.org/10.1002/9780470664797

[5] Jang-Ho Lee, Byoung-Mun Min, & Eung-Tai Kim. (2007). Autopilot design of tilt-rotor UAV using particle swarm optimization method. 2007 International Conference on Control, Automation and Systems. http://dx.doi.org/10.1109/iccas.2007.4406594

[6] Bobela, S. (2016). Thesis title Programme Developing a drone delivery system for blood in Bangalore, India. Global Systems Design Supervisors Niels Gorm Maly Rytter, Lazaros Nalpantidis.https://projekter.aau.dk/projekter/files/230978627/Master_s_thesis_final_Stanislaw_Bobela_GSD.pdf

[7] Rosen, J. W. (2017, June 8). Zipline's ambitious medical drone delivery in africa. MIT Technology Review. https://www.technologyreview.com/2017/06/08/151339/blood-from-the-sky-ziplines-ambitious-medical-drone-delivery-in-africa/

[8] Ersson, L., & Olsson, E. (2020). Drones to the Rescue : A literary study of Unmanned Aerial Systems within healthcare (Dissertation). Retrieved from http://urn.kb.se/resolve?urn=urn:nbn:se:uu:diva-425866

[9] Royall, Paul & Courtney, Patrick. (2019). Medicine delivery by drone - implications for safety and quality. European Pharmaceutical Review. 2019. 103799.

[10] Ministry of Health, Ontario, Canada. (2021). Vaccine Storage and Handling Guidelines. https://www.health.gov.on.ca/en/pro/programs/publichealth/oph_standards/docs/reference/vaccine%20_storage_handling_guidelines_en.pdf

[11] Cohen, V., Jellinek, S. P., Teperikidis, L., Berkovits, E., & Goldman, W. M. (2007). Room-temperature storage of medications labeled for refrigeration. American Journal of Health-System Pharmacy: AJHP: Official Journal of the American Society of Health-System Pharmacists, 64(16), 1711–1715. https://doi.org/10.2146/ajhp060262

[12] U.S. Pharmacopeia. (2017). <659> Packaging and Storage Requirements. https://www.uspnf.com/sites/default/files/usp_pdf/EN/USPNF/revisions/659_rb_notice_english.pdf

[13] Singh, S. P., Burgess, G., & Singh, J. (2008). Performance comparison of thermal insulated packaging boxes, bags and refrigerants for single-parcel shipments. Packaging Technology and Science, 21(1), 25–35. https://doi.org/10.1002/pts.773

[14] Wang, K., Yang, L., & Kucharek, M. (2020). Investigation of the effect of thermal insulation materials on packaging performance. Packaging Technology and Science, 33(6), 227–236. https://doi.org/10.1002/pts.2500

[15] Ackerman, E., & Koziol, M. (2019, April 30). In the Air With Zipline's Medical Delivery Drones. IEEE Spectrum. https://spectrum.ieee.org/in-the-air-with-ziplines-medical-delivery-drones

[16] McCall, B. (2019). Sub-Saharan Africa leads the way in medical drones. The Lancet, 393(10166), 17–18. https://doi.org/10.1016/s0140-6736(18)33253-7

[17] D. P. Raymer, *Aircraft design: A conceptual approach*. Reston: American Institute of Aeronautics and Astronautics, 2021.

[18] PX4 User Guide. (2021). Px4. https://docs.px4.io/master/en/getting_started/px4_basic_concepts.html

[19] [Cavallo, B., "Subsonic Drag Estimation Methods," U.S. Naval Air Development Center, Rept. NADC-A W-6604, 1966.]

[20] Gudmundsson S. General Aviation Aircraft Design - Applied Methods and Procedures. 1st ed. Elsevier; 2014

[21] Sadraey MH. Aircraft Design - A System Engineering Approach. John Wiley & Sons, Ltd; 2013.

[22] Abbott, I., and von Doenhoff, A., Theory of Wing Sections, McGraw-Hill, New York,1949

[23] Bandhu, S. S., & Pamadi, C. (n.d.). Performance, Stability, Dynamics, and Control of Airplanes and Helicopters. : John Wiley & Sons.

[24] J.D. Anderson, "Aircraft Performance and Design," New York, NY, USA: McGraw-Hill, 1999.

[25] [Loftin, Jr., L.K., Subsonic Aircraft: Evolution and the Matching of Size to Performance, NASA Reference Publication 1060, 1980.]

[26] https://rmlh.nic.in

[27] Gabriel Staples, 2013. http://electricaircraftguy.blogspot.com

[28] N. K. Hieu and H. T. Loc, "Airfoil Selection for Fixed Wing of Small Unmanned Aerial Vehicles," *AETA 2015: Recent Advances in Electrical Engineering and Related Sciences*, pp. 881–890, 2016, doi: https://doi.org/10.1007/978-3-319-27247-4_73.

APPENDIX

Figure A. 1: CAD model

Figure A. 2: Side View

Figure A. 3: Top view

Figure A. 4: Front View

Figure A. 6: Tail wheel

Figure A. 5: Payload box

Figure A. 7: Avionics